

Master of Science Thesis in Electrical Engineering
Department of Electrical Engineering, Linköping University, 2024

Power Consumption Modeling of 5G Millimeter-Wave User Equipment

Palatip Jopanya



Master of Science Thesis in Electrical Engineering
Power Consumption Modeling of 5G Millimeter-Wave User Equipment

Palatip Jopanya
LiTH-ISY-EX-24/5663-SE

Supervisor: **Daniel Pérez Herrera**
ISY, Linköpings universitet

Gang Zou
DEVICE COMM RESEARCH, Ericsson

Examiner: **Zheng Chen**
ISY, Linköpings universitet

*Division of Communication Systems
Department of Electrical Engineering
Linköping University
SE-581 83 Linköping, Sweden*

Copyright © 2024 Palatip Jopanya

Abstract

The 5th generation (5G) mobile network has been deployed globally for many years. Compared with Long-Term Evolution (LTE), there are several major improvements, such as throughput, latency, and energy efficiency. The energy efficiency of user equipment (UE) is one of the critical concerns and has been discussed and specified in different updated releases by the 3rd Generation Partnership Project (3GPP) to minimize the UE consumption power. Therefore, it is necessary to understand the behavior of UE power consumption in different network configurations.

In this thesis, the power consumption models of an UE, specifically a millimeter wave (mmWave) UE, are examined. The study was performed in a non-standalone (NSA), where both Long-Term Evolution (LTE) and 5G are connected for dual connectivity. Three modeling methods are investigated: polynomial regression, decision tree regression, and neural network. The results show that the decision tree regression and the neural network are versatile in different test schemes and perform well in prediction, while polynomial regression performs well only with power sweep, i.e., the simple curve of the target variable. Moreover, adding a few highly correlated features improves the performance of the model.

Acknowledgments

I would like to express my sincere gratitude to Gang Zou, my supervisor at Ericsson, for his continuing support guidance, and insightful discussions throughout the course of the thesis. I also would like to express my sincere gratitude to Zheng Chen, my examiner at Linköping University, for her guidance and constant tracking of the progress of my thesis, and to Daniel Pérez Herrera, my supervisor at Linköping University, for his guidance in thesis writing, data analysis, and visualization.

Furthermore, I would like to thank Henric Sundelin, Mikael Höglund, and Jens Kongstad in the laboratory for their support in facilitating the laboratory environment and laboratory access. I also would like to thank Raihan Rafique for his constructive suggestions.

Finally, I want to thank my family for the encouragement and their unwavering love that has been a source of motivation.

Contents

Notation	ix
1 Introduction to 5G ENDC and Motivation	1
1.1 5G FR2 (mmWave) Massive MIMO System	2
1.2 Aim	2
1.3 Research Questions	2
1.4 Previous Studies	3
1.5 Limitations	3
2 Test and Environment Setup	5
2.1 User Equipment (UE)	5
2.2 Radio Network Emulator and Chamber	5
2.3 Robotic Gimbal	7
2.4 Power Supply and Monitoring Tool	8
3 Measurements and Data Collection	11
3.1 Baseline Parameters	11
3.2 DUT Orientation	11
3.3 LTE Idle Mode Power Measurement	13
3.4 Connected Mode: LTE-only Power Measurement	14
3.4.1 LTE-only RF Uplink Power Sweep	14
3.4.2 DUT Horizontal Sweep	15
3.5 Connected Mode: ENDC Power Measurement	17
3.5.1 NR Uplink RF power sweep	17
3.5.2 NR Downlink RF Power Sweep	19
3.5.3 DUT Orientation Sweep	20
3.6 Polar Plots of RSRP in LTE and NR	20
4 Method	25
4.1 Polynomial Regression	25
4.2 Decision Tree Regression	26
4.3 Neural Networks	27

5 Modeling and Performance	31
5.1 Generic States Transition	31
5.1.1 RRC States	31
5.2 Loss in Wireless Tranmission	33
5.3 Different Methods in UE Power Modeling	33
5.4 Modeling in Idle Mode	35
5.5 Single Connectivity and Dual Connectivity Modeling in Connected Mode	35
5.5.1 Single and Multiple Features Polynomial Regression	35
5.5.2 Single and Multiple Features Using Decision Tree Regression	39
5.5.3 Multiple Features Using Neural Network	42
5.6 Prediction System	48
6 Results	53
7 Conclusion	55
7.1 Findings in Modeling	55
7.2 Discussion	56
7.2.1 Research Questions	56
7.2.2 Further Research	56
Bibliography	59
Index	60

Notation

ABBREVIATIONS

Shortening	Meaning
3GPP	3rd Generation Partnership Project
5G	5th Generation Mobile Network
5GCN	5G Core Network
CA	Carrier Aggregation
CRS	Cell-specific Reference Signal
DL	Downlink
DRX	Discontinuous Reception
DUT	Device Under Test
ENDC	Eutra-NR Dual Connectivity
FR2	Frequency Range 2
LNA	Low Noise Amplifier
LTE	Long Term Evolution
MCS	Modulation Coding Scheme
MMWAVE	Milimeter-Wave
NR	New Radio
PA	Power Amplifier
RF	Radio Frequency
RRC	Radio Resource Control
UE	User Equipment
UL	Uplink

1

Introduction to 5G ENDC and Motivation

The technical specifications of the cellular modem, i.e. User Equipment (UE) in 3GPP standards, have continually evolved to become more computationally powerful every year. It is also expected to perform well both in throughput and latency since these factors are closely related to power consumption in the UE, and there are always trade-offs between latency, throughput, and energy efficiency in the UE. This draws attention to the understanding of the UE power consumption model. This thesis will primarily focus on investigating the power consumption of a 5G, also called New Radio (NR), cellular modem in a smartphone while disregarding power consumption of other components such as the application processing unit, background applications, screen, WiFi, Bluetooth, GPS etc.

Long-Term Evolution (LTE) has undergone a long development journey since its first specification, Release 8, in 2009, and has reached maturity over time. The first 5G specification, on the other hand, was released in 2017, Release 15, while LTE continues to be developed in parallel with 5G, as it remains an important component of 5G Non-Standalone (NSA). This thesis will focus on the 5G NSA option 3a, as shown in Figure 1.1, for network-side setup. NSA option 3a has been widely deployed in the transition period toward 5G because it allows fast implementation by using legacy Evolved Packet Core (EPC) therefore less capital in investment for the 5G Core Network (5GCN). This type of setup (5G NSA) is also called Eutra-NR dual connectivity (ENDC). In addition, ENDC is widely used because it provides the benefit of dual connectivity by offering large coverage in the sub-6 GHz band of LTE and generous bandwidth resources in Frequency Range 2 (FR2) in NR to boost UE throughput.

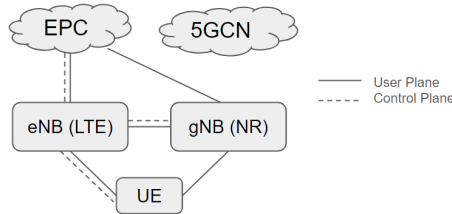


Figure 1.1: NSA option 3a network topology.

1.1 5G FR2 (mmWave) Massive MIMO System

In NR, FR2 lies between 26.5 and 71 GHz. A FR2 base station contains multiple mmWave antenna arrays which are used to facilitate beamforming and steering capabilities by manipulating phases and amplitudes and exploiting a large number of antenna elements. At the UE side, each of the mmWave antenna arrays, i.e. antenna panel, is located at different locations in the UE. The array consists of multiple antenna elements, for example, a 1x5 dual-polarized antenna array. With an antenna array, the UE can achieve better channel conditions from a beam radiation and can also transmit a directive beam toward the base station.

1.2 Aim

The main focus of this thesis is to model the power consumption of 5G UE. A 5G NSA network was emulated with a radio network emulator to facilitate connectivity for LTE and NR. Various test cases were performed, and power consumption data was collected from both the network emulator and the UE. The aim of this thesis is to investigate modeling methods using measurement data from the UE and the network emulator. Additionally, the results provide insights into UE power consumption in different network settings and test scenarios.

1.3 Research Questions

Here are the research questions that are stated to align the thesis with its goals. The answers are provided in the conclusion.

1. How can features be selected for each test scheme, and will that improve the models with more features?
2. What is the performance of each modeling method in each test scheme?
3. How can one build a potential prediction system for 5G UE power consumption?

1.4 Previous Studies

There were studies about UE power modeling. A study shows that the model can be divided into two parts: baseband power and radio frequency (RF) power. The uplink (UL) transmitted power, the downlink (DL) sensitivity, and the Modulation and Coding Scheme (MCS) are found to be closely linked to UE power consumption [4] therefore, they are used in power consumption models. The UL transmission power and the DL sensitivity reflect the power consumption of RF chains such as the power amplifier (PA) and low noise amplifier (LNA). The MCS and throughput are linked to the baseband power used for modulation and channel coding/decoding.

A study shows that there is an improvement of roughly 38 percent in energy efficiency (EE) in the transition between the 1st and 2nd generation UEs that were made in 2012 and 2013 respectively [5]. The EE indicates the amount of energy used to transfer a byte of data. In addition, an increase in throughput by a factor of 10 will increase power by 10 percent [5].

A study on power consumption in carrier aggregation (CA) in LTE-Advance shows that CA improves power saving by 31 percent when the throughput is doubled and the transmission file is large [2]. File size matters here because higher throughput can quickly finish transmission and turn UE into sleep mode.

A study shows that switching from single input single output (SISO) to 4x4 multiple input multiple output (MIMO) at the UE terminal requires only 10 % more power from SISO to facilitate 4x4 MIMO at the UE terminal [1]. However, in this thesis, SISO is used on the base station side due to the limitation in base station antennas in the test setup.

A study on reducing unnecessary periodic symbols, the Cell Specific Reference Signal (CRS), when there is no UE schedule packet in the network. This reduces power not only at base stations but also on the UE side [3].

1.5 Limitations

All test cases in this thesis are limited to the following aspects. The effect in UE power of different temperatures in UE is not included in this study. The test chamber has no obstacles and has non-reflective walls. Therefore, the signal is assumed to be in line of sight (LOS) and has a limited effect from the multipath propagation. The distance between the UE and the base station antennas is assumed to be fixed in all possible orientations of the gimbal.

2

Test and Environment Setup

Presently, ENDC is widely deployed. Legacy lower frequency LTE is used as an anchor for control channel to provide wide coverage, while NR at higher frequencies, specifically FR2, is used to boost throughput in dense area. In this thesis, ENDC is configured. A Sony Xperia 1 mark 4 is the main UE used in most test schemes, and a Sony Xperia 1 mark 5 is used for the comparison in the idle case between two models.

2.1 User Equipment (UE)

The setup on the network side to support Sony Xperia 1 Mark 4 is a paired spectrum of 10 MHz at band b5 (850 MHz) in LTE in FDD mode and an unpaired spectrum of 100 MHz at band n260 (38 GHz) in NR in TDD mode. The batteries in the UEs were removed. The power cables were then soldered to the UE battery connector as in Figure 2.1. This is for connection to the power supply.

Most likely, there are multiple antenna panels located in different parts of the UE. One of the mmWave antenna panels can be observed on the back of the Sony Xperia 1 mark 4. It is a dual-polarized 5x1 mmWave antenna panel for NR as shown in Figure 2.2.

In the tests, the screen is turned off, and unnecessary functions are turned off throughout all test cases in this thesis.

2.2 Radio Network Emulator and Chamber

The radio network emulator, CMX500 from Rohde and Schwartz, is used to configure and generate the signal on the network side as in Figure 2.3. There are 2

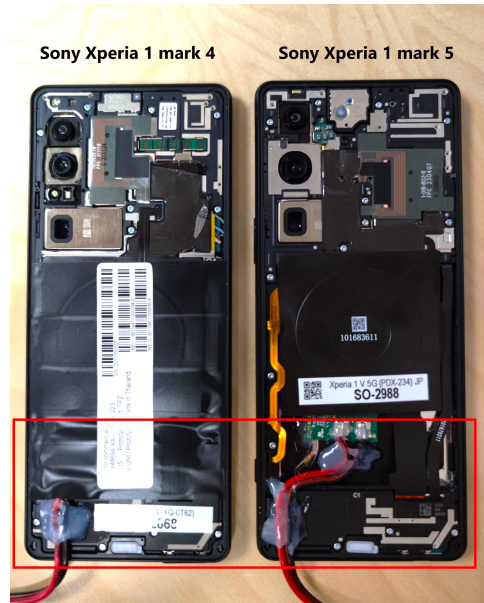


Figure 2.1: Batteries were removed and cables were soldered in Sony Xperia 1 mark 4 and 5.

ports dedicated for NR FR2, one for horizontal polarization and the other one for vertical polarization. The same applies to FR1 of LTE, one for the main polarization and one for the diversity polarization.

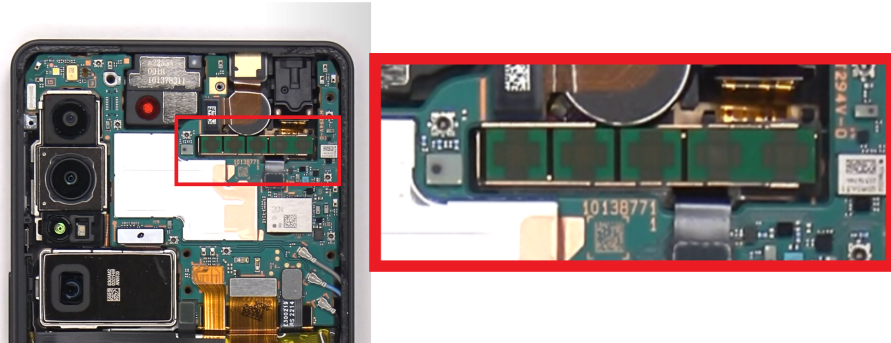


Figure 2.2: Dual polarized 5x1 mmWave antenna panel for NR FR2.



Figure 2.3: R&S CMX500 Network Emulator.

The RF feeder is connected from the CMX500 to two horn antennas inside the chamber as in Figure 2.4. The UE is mounted on the robotic gimbal which is programmable to rotate in both horizontal and vertical directions. The whole setup is presented in the diagram in Figure 2.5.

The graphic user interface (GUI) of the radio network emulator is shown in Figure 2.6. All cell parameters can be configured through the emulator.

2.3 Robotic Gimbal

The robotic gimbal is used to control the orientation of the UE so that the UE can have a different angle facing the base station antennas. It can also be used for the case that the UE needs to sweep around the different direction in horizontal or vertical orientation to measure the quality of the received signal in all 360 degrees. Figure 2.7 shows that the UE is mounted at $H = 0$ degree.

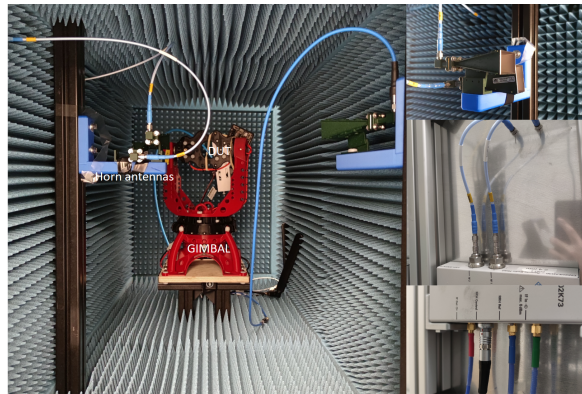


Figure 2.4: Clockwise: the chamber, horn antennas, and RF ports.

2.4 Power Supply and Monitoring Tool

The power for the device under test (DUT) is supplied b via cables by the Monsoon power monitor from the Monsoon solution as in Figure 2.8. It can be configurable for the voltage and size of the battery in mAh. The power monitor is connected to the local computer to log the UE power. The maximum sampling rate of power measurement is 5000 samples per second.

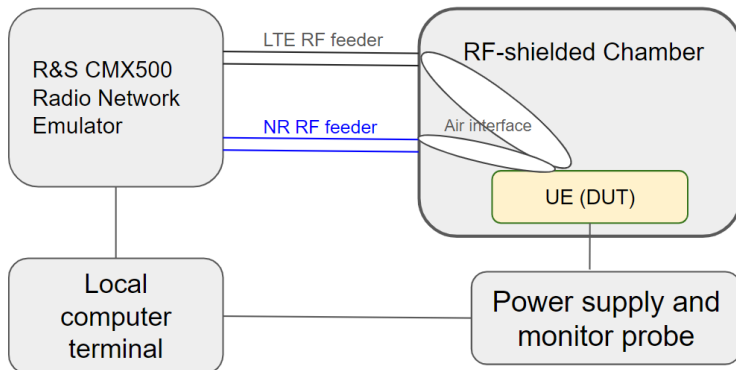


Figure 2.5: Test setup diagram

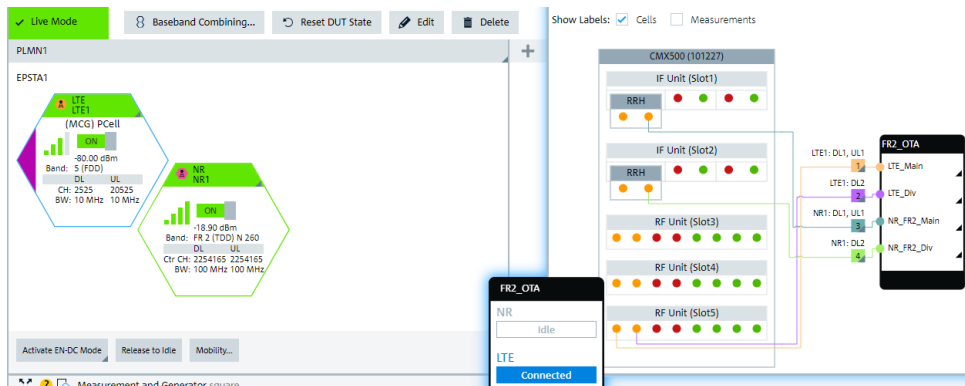


Figure 2.6: GUI of radio emulator.

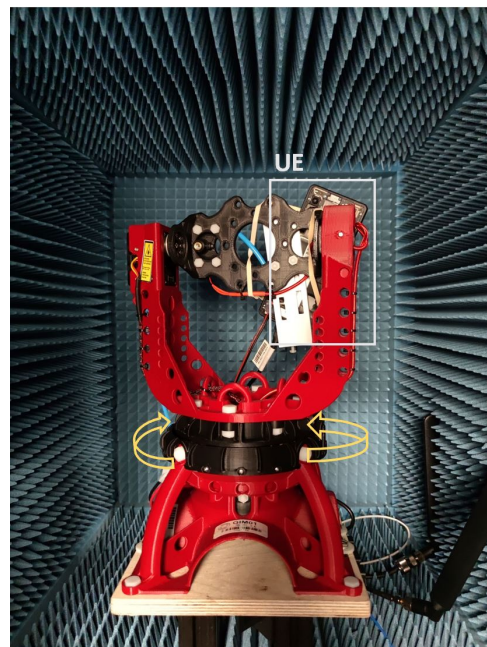


Figure 2.7: UE is mounted at H=0 degree.



Figure 2.8: Monsoon Power monitor is used for supplying UE power and UE power logging

3

Measurements and Data Collection

3.1 Baseline Parameters

Baseline parameters are the set of values in the configuration of the radio network emulator. The test schemes are the specific set of settings that is used to learn the UE power consumption. Each test scheme will have its specific setting that is partially different from the baseline values. There are different combinations in band in the UE capability for dual connectivity as shown in Table 3.1. The baseline for Sony Xperia 1 Mark 4 is shown in the Table 3.2.

The power data from Monsoon power monitor and the network emulator CMX500 log data are extracted and post-processed into a simplified csv format.

3.2 DUT Orientation

UE is mounted on the gimbal and its posture is adjustable in horizon in degrees. Figure 3.1 shows the orientation on the horizon in degrees, H (degree), which measures the angle of the backside of the UE toward the base station antennas. The vertical orientation is always fixed at 0 degrees in the study to simplify the complexity of the model.

Table 3.1: UE capabilities for ENDC

Band combination supported for ENDC
Sony Xperia 1 Mark 4 LTE B5 with NR band n260
Sony Xperia 1 Mark 5 LTE B1 with NR band n257

Table 3.2: Baseline parameters for Mark 4

LTE parameters and values	NR parameters and values
Carrier frequency Duplex: FDD LTE band 5 Bandwidth: 10 MHz E-ARFCN DL: 2525 E-ARFCN UL: 20525 Carrier frequency DL: 881.5 MHz Carrier frequency UL: 836.5 MHz	Carrier frequency Duplex: TDD NR band 260 Bandwidth: 100 MHz Subcarrier spacing (SCS): 120 kHz NR-ARFCN: 2254165 Carrier center: 38499.96 MHz
Downlink power (Cell Tx power) Max Cell Power: -52.2 dBm Uplink power (UE Tx power) TCP: Closed loop Target Power Total RMS: 0 dBm	Downlink power (Cell Tx power) Total Cell Power: 10.1 dBm Uplink power (UE Tx power) TCP: Closed loop Target Power Total RMS: 0 dBm
UE scheduling Transmission mode (TM): TM1: Single Antenna	MIMO layer in NR Single beam with 2 horn antennas
MCS for RMC scheduling MCS table: 64QAM QPSK MCS: UL=5, DL=5 64QAM MCS: UL=27, DL=26	MCS for RMC scheduling MCS table: 64QAM QPSK MCS: UL=2, DL=4 64QAM MCS: UL=19, DL=19

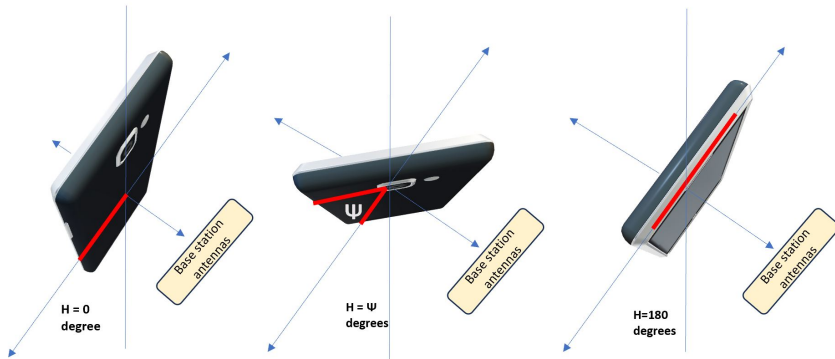


Figure 3.1: Orientation in horizon in degrees.

3.3 LTE Idle Mode Power Measurement

In UE idle mode, Radio Resource Control (RRC) is in idle state (RRC_IDLE), where UE listens to the network periodically. This is defined by a parameter called the *paging cycle*. It tells the length between 2 "ON" durations, where "ON" means UE is listening to network so the receiver is active to monitor paging from network, and "OFF" means UE is in sleep mode. The measurements of idle mode are shown in Figure 3.2 with different paging cycles of 320, 640 and 1280 ms, respectively. Figure 3.3 shows a comparison of UE power in idle mode between Mark 4 and Mark 5. The power in paging is reduced for about 40 mW in Mark 5 compare it with Mark 4. The power costs for each UE are shown in Table 3.3

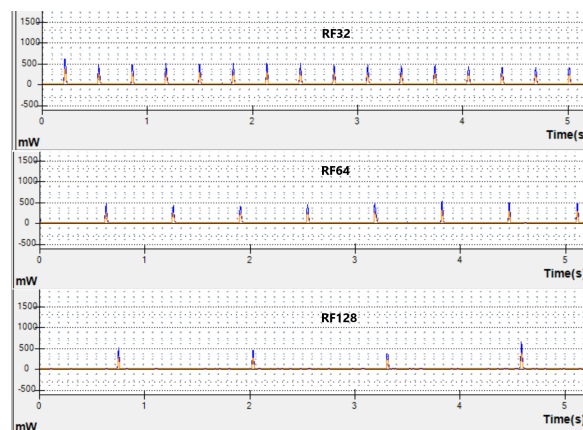


Figure 3.2: Idle mode in different paging cycles of Mark 4.

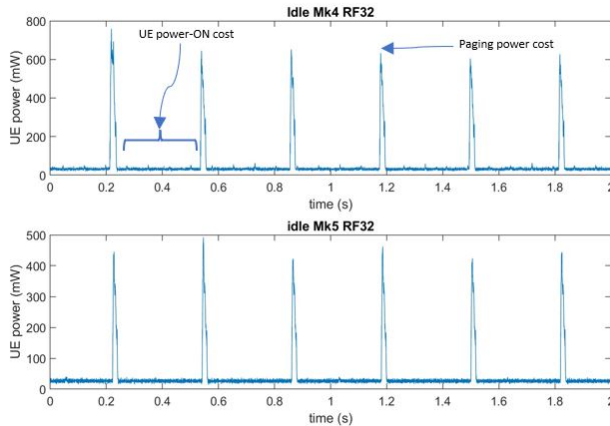


Figure 3.3: UE power-on and paging power cost in idle mode

Table 3.3: Power cost in idle mode

Power cost in idle mode, RF32
Sony Xperia 1 Mark 4
Sleep mode power cost = 31.2
Mean power in idle mode ($P_{idle,Mk4}$) = 53.1 mW
Sony Xperia 1 Mark 5
Sleep mode power cost = 26.1
Mean power in idle mode ($P_{idle,Mk5}$) = 40.1 mW

3.4 Connected Mode: LTE-only Power Measurement

3.4.1 LTE-only RF Uplink Power Sweep

In this scheme, the UE uplink transmission power is swept between -9 and 23 dBm, it is located in the fixed position and always schedules packets with QPSK modulation on both the uplink and the downlink in LTE. The uplink transmission power is controlled by the network emulator to observe the measurement values. Three DUT positions in horizontal orientation: H = 0, H = 60 and H = 90 degrees relative to the horizon as in Figures 3.4, 3.5 and 3.6, respectively. At 0 degree, the antenna panel is located approximately at boresight of the downlink transmitted signal from the base station. The correlation heatmap for the case at 0 degrees is shown in Figure 3.7. From the result, it is clear that the LTE uplink power is highly correlated with the UE power which is reasonable.

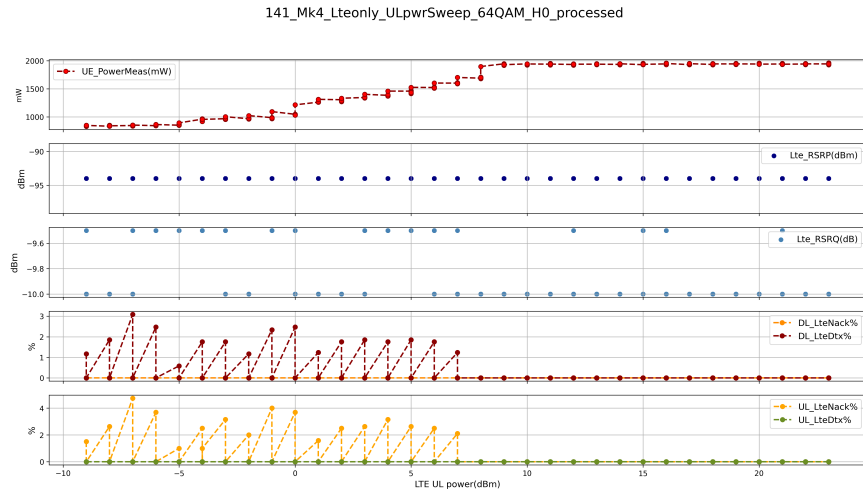


Figure 3.4: Uplink power sweep in LTE-only with 64QAM at $H=0$ degree.

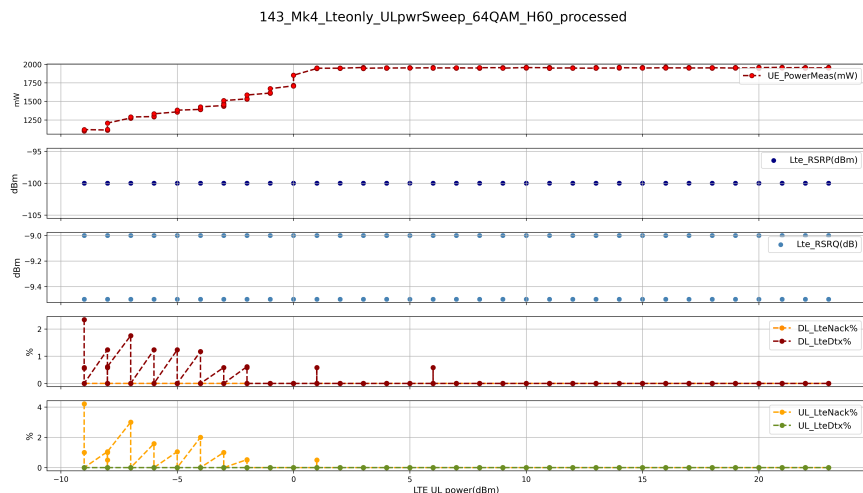


Figure 3.5: Uplink power sweep in LTE-only with 64QAM at $H=60$ degree.

3.4.2 DUT Horizontal Sweep

In this scheme, a DUT is swept between -180 and 180 degrees in horizon. During the test, the UE is always scheduling packets with QPSK and 64QAM modulation on both the uplink and downlink in LTE. The measurement results are shown in Figures 3.9 and 3.10, respectively. The correlation heatmaps of both cases are shown in Figures 3.11 and 3.12, respectively. Although the highest correlation coefficient is not so strong in the QPSK case, it can be effect from long data series because it is obvious that RSRP (dBm) is going together as the UE power in some

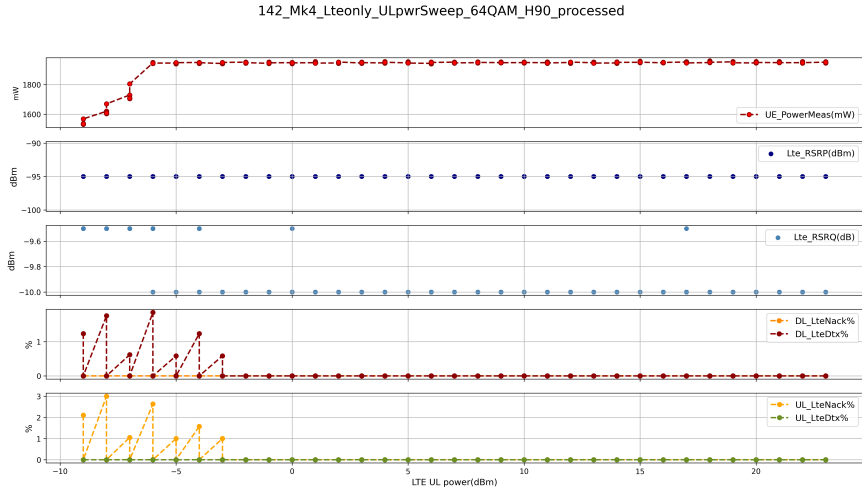


Figure 3.6: Uplink power sweep in LTE-only with 64QAM at H=90 degree.

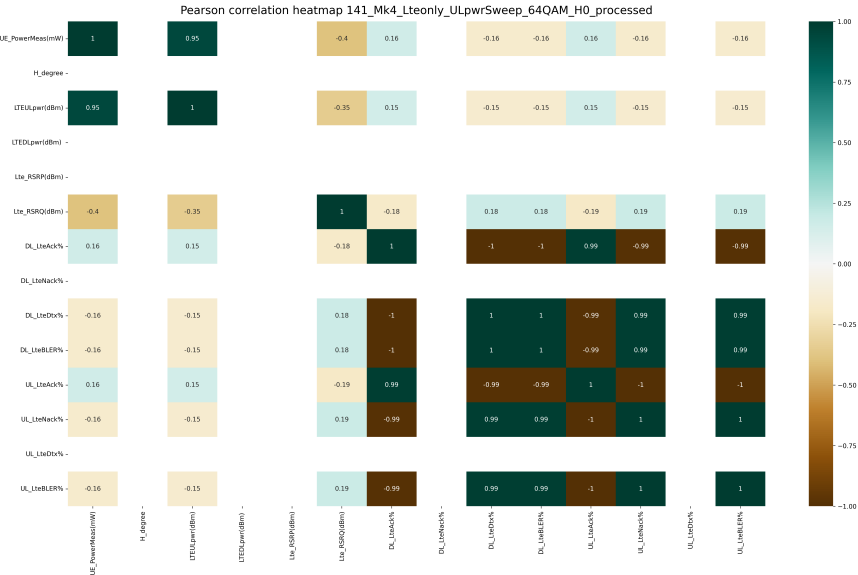


Figure 3.7: A sample of correlation matrix heatmap of uplink power sweep in LTE-only with 64QAM at H=0 degree.

range of the sweep but not always. In 64QAM case, at some certain orientation, after 40 degrees, the NACK (%) starts to appear, and this affects the UE power curve compared to QPSK case which always gives zero in NACK (%) and DTX (%).

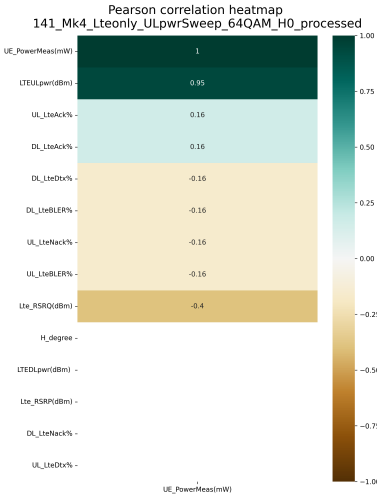


Figure 3.8: A correlation heatmap of uplink power sweep in LTE-only with 64QAM at H=0 degree.

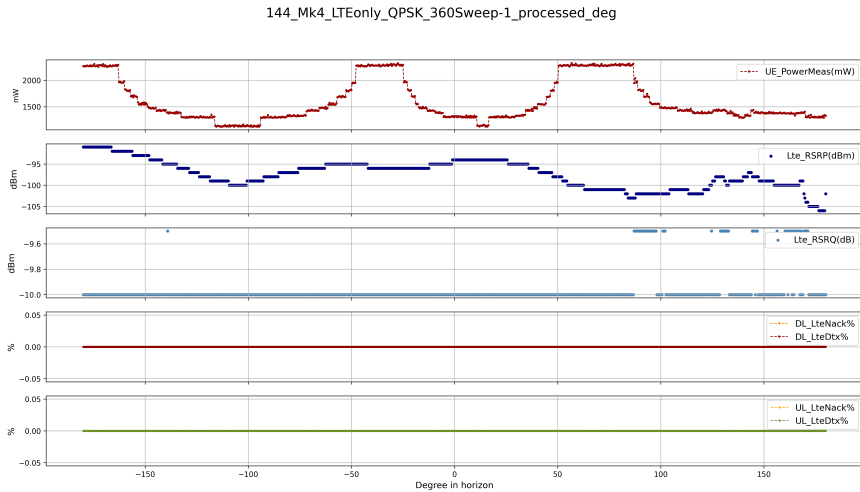


Figure 3.9: Horizontal sweep between -180 and 180 degrees in LTE-only with QPSK.

3.5 Connected Mode: ENDC Power Measurement

3.5.1 NR Uplink RF power sweep

In this scheme, the UE uplink power is swept between -39 and 23 dBm, and the DUT is located in the fixed position at H = 112 degrees, and it always schedules packets with 64QAM modulation in both UL and DL in LTE and QPSK in both

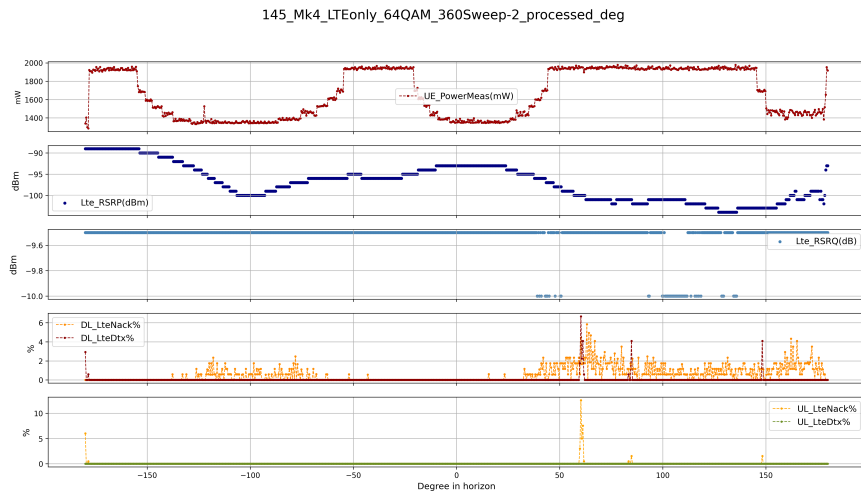


Figure 3.10: Horizontal sweep between -180 and 180 degrees power sweep in LTE-only with 64QAM.

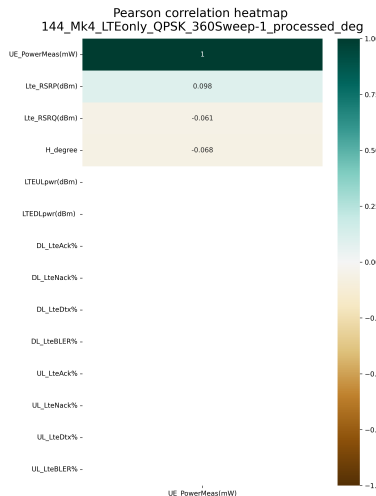


Figure 3.11: A correlation heatmap of horizontal sweep between -180 and 180 degrees power sweep in LTE-only with QPSK.

UL and DL in NR as in Figure 3.13. The correlation heatmap is shown in Figure 3.14. From the heatmap, it is clear and reasonable that the NR uplink power (dBm) is highly correlated to the UE power.

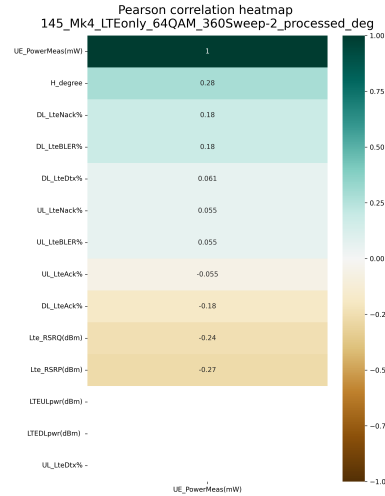


Figure 3.12: A correlation heatmap of Horizontal sweep between -180 and 180 degrees power sweep in LTE-only with 64QAM.

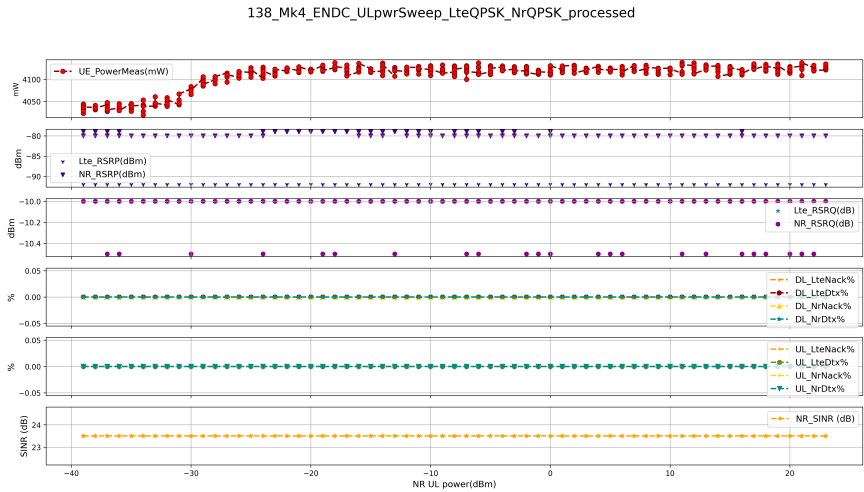


Figure 3.13: NR uplink power sweep in ENDC with 64QAM in LTE and QPSK in NR.

3.5.2 NR Downlink RF Power Sweep

In this scheme, UE is located at the fixed position at $H = 112$ degrees and is always scheduling packets at 64QAM modulation in both UL and DL in LTE and 64QAM in both UL and DL in NR. Figure 3.15 shows the measurement results. The correlation heatmap is shown in Figure 3.16. From the measurement, it is clear and reasonable that SINR (dBm) and RSRQ (dBm) are highly correlated to

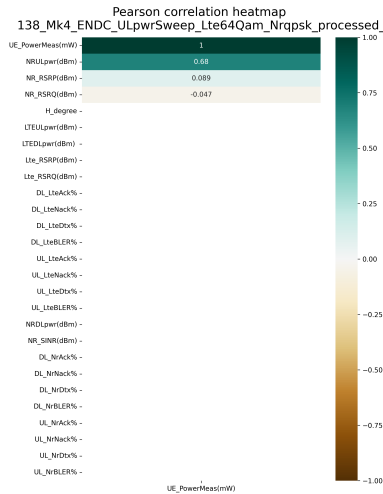


Figure 3.14: Correlation heat map of NR uplink power sweep in ENDC with 64QAM in LTE and QPSK in NR.

the UE power.

3.5.3 DUT Orientation Sweep

In this scheme, DUT is swept between 0 and 180 degrees in the horizon. Figure 3.17 shows the measurement results in which UE is always scheduling packets with 64QAM in LTE and QPSK in NR. Figure 3.18 shows the measurement results show UE is always scheduling packets at MCS = 64QAM in both UL and DL in LTE and NR. The correlation heatmaps are shown in Figures 3.19 and 3.20. From the result, it can be said that most of the time the UE power is flat except when there is high NACK (%) in either uplink or downlink in NR then the UE power is low. This is also reflected in the correlation heatmap which shows that the percent NACK is highly negatively correlated to the UE power.

3.6 Polar Plots of RSRP in LTE and NR

Polar plot is a kind of data visualization for the received power level in circle form. In Figures 3.21 and 3.22 show the UE received power level of LTE and NR in QPSK and 64QAM, respectively.

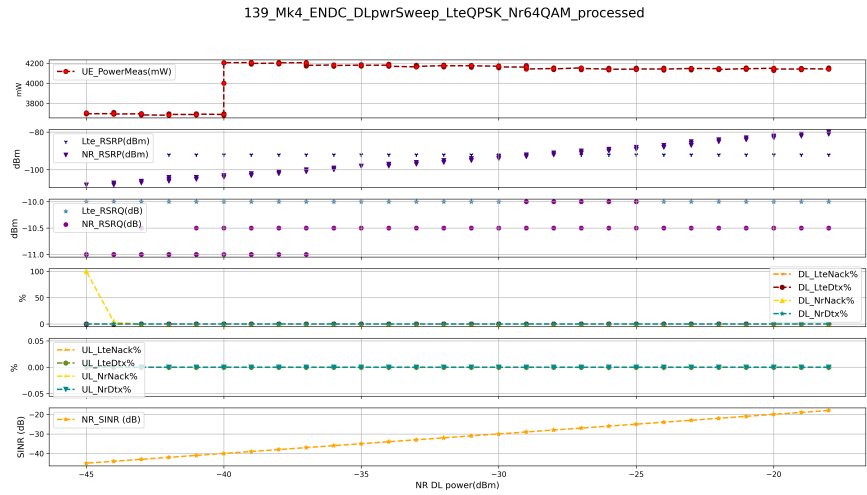


Figure 3.15: NR downlink power sweep in ENDC with 64QAM in LTE and 64QAM in NR.

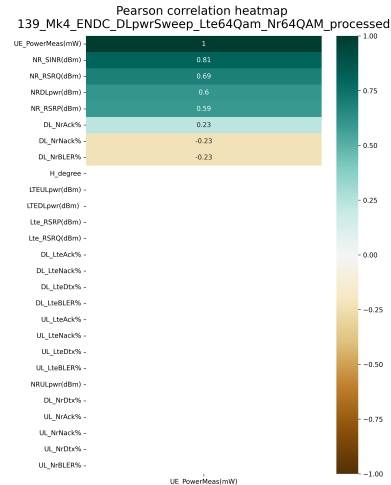


Figure 3.16: Correlation heatmap of NR downlink power sweep in ENDC with 64QAM in LTE and 64QAM in NR.

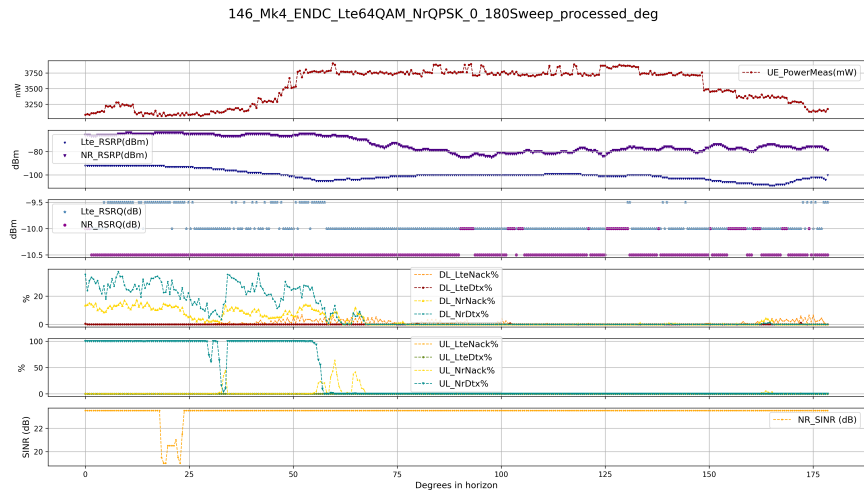


Figure 3.17: Horizon sweep between 0 and 180 degree in ENDC with 64QAM in LTE and QPSK in NR.

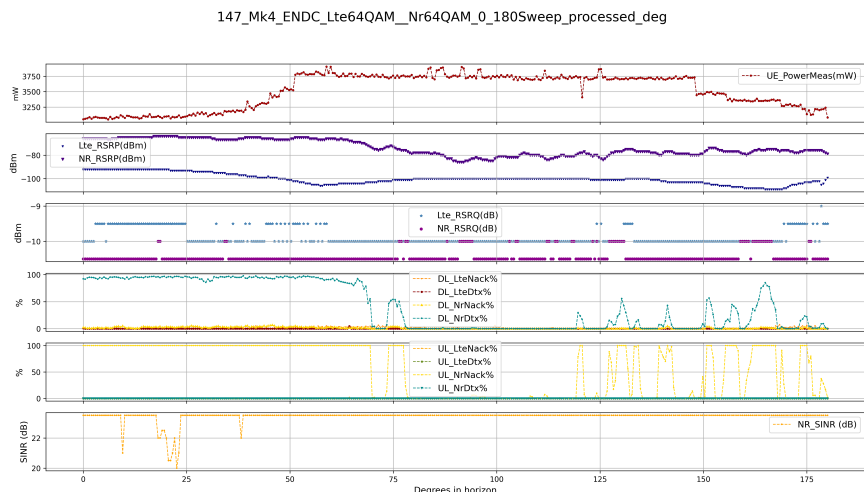


Figure 3.18: Horizontal sweep between 0 and 180 degree in ENDC with 64QAM in both LTE and NR.

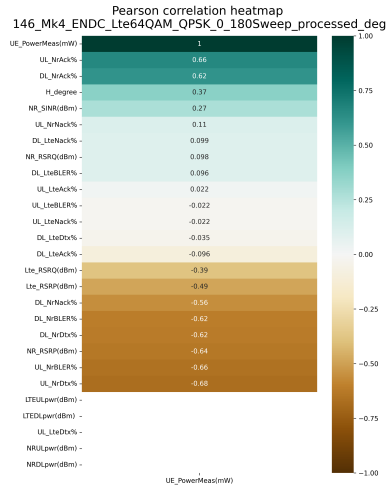


Figure 3.19: Correlation heatmap of horizontal sweep between 0 and 180 degree in ENDC with 64QAM in LTE and QPSK in NR.

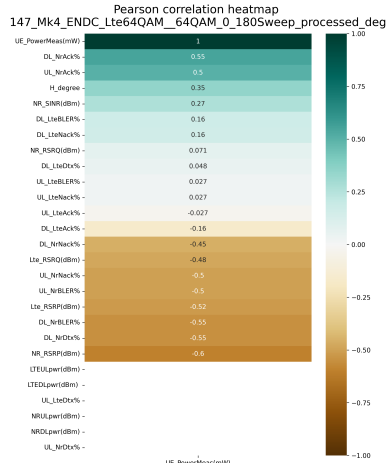


Figure 3.20: Correlation heatmap of horizontal sweep between 0 and 180 degree in ENDC with 64QAM in both LTE and NR.

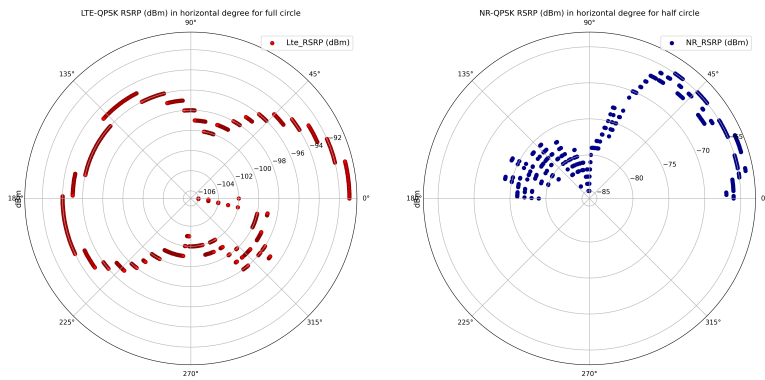


Figure 3.21: Polar plot of RSRP of QPSK for full circle in LTE and for half circle in NR.

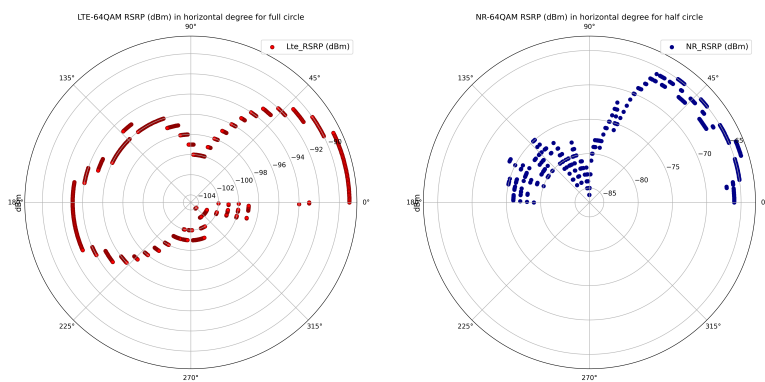


Figure 3.22: Polar plot of RSRP of 64QAM for full circle in LTE and for half circle in NR.

4

Method

Three modeling methods are used in this thesis, namely polynomial regression, decision tree regression, and neural network. The theory of each method is described below.

4.1 Polynomial Regression

Polynomial regression is a special type of linear regression estimator that applies the multiplication of dependent variables in linear regression. Given that X is an independent variable as a matrix size of $m \times q$ and Y is a dependent variable as a vector size of $m \times 1$, the data have m samples, p features, and q number of polynomial terms. It can be modeled as

$$Y = X\beta + \epsilon,$$

where β is a bias vector and ϵ is an error. The objective is to find $E[Y|X]$ or \hat{Y} . A dataset X can be denoted as $x_i = (x_{i1}, x_{i2}, x_{i3}, \dots, x_{ip})$, where $i = 1, 2, \dots, m$. y_i in the polynomial regression of n^{th} order can be expanded to

$$y_i = \beta_0 + \sum_{j=1}^p \beta_j x_{ij} + \sum_{j=1}^p \sum_{k=j}^p \beta_{jk} x_{ij} x_{ik} + \sum_{j=1}^p \sum_{k=j}^p \sum_{l=k}^p \beta_{jkl} x_{ij} x_{ik} x_{il} + \dots$$

Solving for β :

$$\beta = (X^T X)^{-1} X^T Y.$$

The total number of combinatorial terms, q , of degree n^{th} and p features can be derived as

$$\sum_{k=0}^n \binom{k+p-1}{k}.$$

For example, 3 features, x_1, x_2, x_3 , and 2^{nd} order will have a total of 10 combinatorial terms as

$$\hat{y} = \beta_0 + \beta_1 x_1 + \beta_2 x_2 + \beta_3 x_3 + \beta_{11} x_1^2 + \beta_{12} x_1 x_2 + \beta_{13} x_1 x_3 + \beta_{22} x_2^2 + \beta_{23} x_2 x_3 + \beta_{33} x_3^2.$$

r2 score is the performance indicator, and is derived as

$$r2_score = 1 - \left(\frac{SS_r}{SS_t} \right),$$

where SS_r is the sum square of residual, it is derived as

$$SS_r = \sum_i (y_i - \hat{y}_i)^2.$$

SS_t is sum square of the Euclidean distance between each value and the mean, it can be denoted as

$$SS_t = \sum_i (y_i - \bar{y})^2.$$

r2 score lies between -inf and 1 where 1 means the best possible prediction performance.

The following subsections will show the results of the polynomial regression of each scheme.

4.2 Decision Tree Regression

Decision tree regression is used to estimate continuous or discrete input in the form of discrete target values, i.e., subsets of output. Decision tree regression can capture non-linear relationships by splitting the data into subsets and fitting simple models to these subsets.

The leaves represent class labels, child nodes that show target value. The branches are the conjunctions of input variables, features, that direct to different class labels. A sample decision tree can be seen in Figure 4.1.

The algorithm of the decision tree regression is based on the expected information gain (I), also called mutual information between the entire data set M and the potential child set N. It is derived as

$$\mathbb{E}\{I(M, N_i)\} = H(M) - H(M|N).$$

Where $H(M)$ is an entropy of the parent node that derived as

$$H(M) = - \sum_i p_{M_i} \log_2 p_{M_i}.$$

and $H(M|N)$ is a weighted sum of entropies of the child set N that is derived as

$$H(M|N) = \sum_i p_{N_i} \sum_j -P(M_j|N_i) \log_2 P(M_j|N_i).$$

It compares the information gain of each split of each tree, feature. The split that gives the highest information gain will be used in the decision tree, and the process continues until the information gain is zero or the depth of the branch has reached the maximum depth.

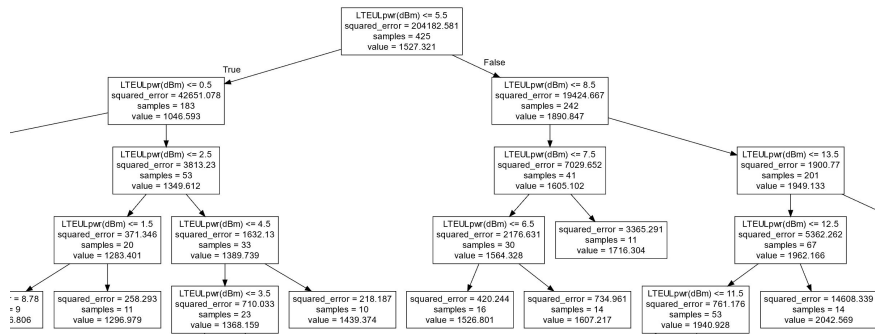


Figure 4.1: An example of decision tree.

4.3 Neural Networks

In a neural network, the target variable is denoted as an output. The features are the input of the neural network, and each link has its own weight. For example, a 2 hidden layer neural network diagram can be seen in Figure 4.2.

The hyperparameters for the neural network in this thesis are defined as follows. The number of features is between 3 and 4, the number of output is 1, the number of hidden layers is 2, the dense in the first and second hidden layers is 64, the epoch is 1000, and the activation function is a rectified linear unit.

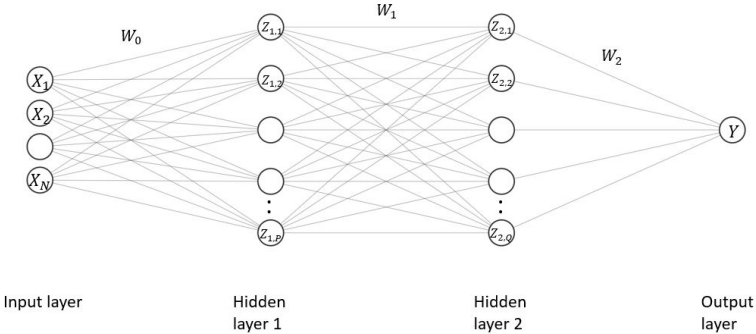


Figure 4.2: A 2-hidden-layer neural network diagram.

The single-output, multiple-input, j^{th} hidden-layer of deep neural network can be derived in simplified form (vector and matrix form) as

$$\hat{y} = g(W_{0,j} + W_j^T Z_j),$$

where \hat{y} is a target variable, $W_{0,j}$ is a constant weight in the j -th layer, W_j is a vector of weights in the j -th layer, Z_j is a vector of nodes z in the j -th layer and $g(\cdot)$ is an activation function. The vector of nodes in any hidden layer i^{th} , Z_i , can be derived as

$$Z_i = W_{0,i-1} + W_{i-1}^T Z_{i-1},$$

where Z_{i-1} is a vector of nodes Z in the $i^{th}-1$ layer, $W_{0,i-1}$ is a constant weight vector in the $i^{th}-1$ layer in the $i^{th}-1$ layer, W_{i-1} is a weight matrix such that each row is a vector of weight out of each node in the $i^{th}-1$ layer, and Z_{i-1} is a vector of nodes in the $i^{th}-1$ layer.

This will be repeated until the first hidden layer, where it can be derived as

$$Z_1 = W_{0,0} + W_0^T X,$$

where X is the input vector of the feature. The initial weights are generated at random at first, it is then used for calculating the gradient. A small step of gradient is used toward the descent direction of the gradient, then all weights are updated. These steps will be repeated until the weights converge. Performance can be derived using mean squared error (MSE) loss as

$$MSE(W) = \frac{1}{N} \sum_{i=1}^N (y_i - \hat{y}(x_i; W))^2,$$

where $MSE(W)$ is the mean squared error as a function of weight W , N is the size of input, y_i is the actual target value and $\hat{y}(x_i; W)$ is the estimated value

based on weight W and input X_i . Similarly in regression, the r2 score is a good measure to have the same performance matrix in all the investigated methods.

5

Modeling and Performance

5.1 Generic States Transition

5.1.1 RRC States

RRC refers to a layer 3 control plane protocol that connects UE and the base station. Figure 5.1 shows the protocol for the RRC connection. There are three RRC states in NR: RRC_IDLE, RRC_INACTIVE, and RRC_CONNECTED. In LTE, there were only RRC_IDLE, RRC_CONNECTED. However, in Release 16 RRC_ACTIVE was introduced in LTE. Figure 5.2 shows the transition possibility in RRC state.

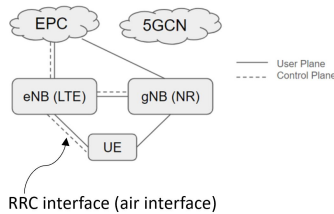


Figure 5.1: RRC in the radio access network topology

In this thesis, RRC_IDLE will be used to refer RRC_IDLE and RRC_INACTIVE, the situation in which UE has no RRC connection. This is to simplify the term, since both states are in a deep sleep mode and consume approximately identical UE power. The improvement with RRC_INACTIVE is a faster and more efficient resumption to RRC_CONNECTED state [6].

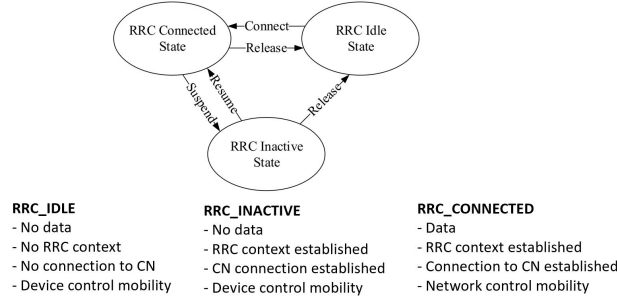


Figure 5.2: RRC states transition possibility and description

In connected mode, there are three schemes to be considered, namely the RRC_CONNECTED without any scheduled data, RRC_CONNECTED with only LTE scheduled data, and RRC_CONNECTED with both LTE and NR scheduled data (ENDC). The RRC_CONNECTED mode without any scheduled data, in this scheme, UE applies the Connected-mode Discontinuous Reception (C-DRX) power saving scheme, which means UE will constantly listen to the PDCCH for an interval of "C-DRX-ON" duration, and UE will not listen to the network and reduced power consumption for an interval of "C-DRX-OFF" duration. A C-DRX cycle is defined as one "C-DRX-ON" followed by one "C-DRX-OFF". After a certain period of time, inactivity timer, which is multiple C-DRX cycles without any schedule data, UE will turn into idle mode. All RRC states and transitions and a generic view of the UE power can be seen in Figure 5.3.

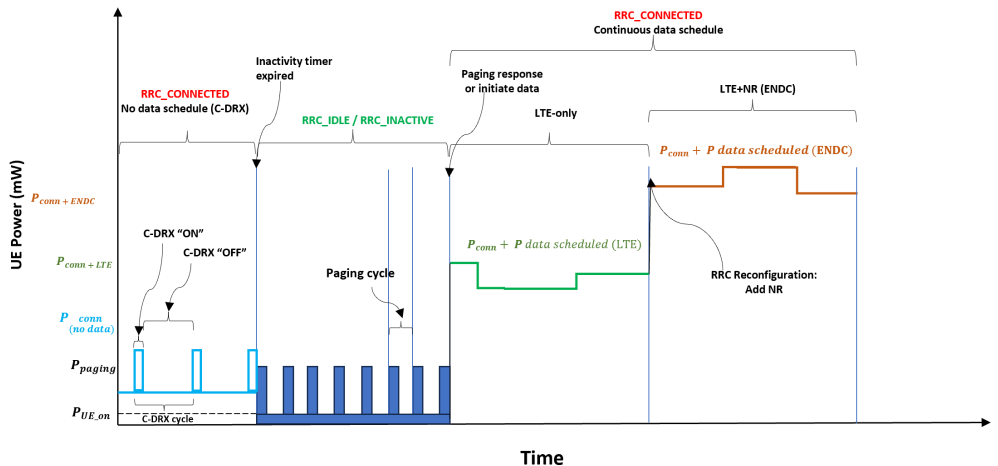


Figure 5.3: Generic states, transition, and UE power.

5.2 Loss in Wireless Tranmission

In free-space pathloss, the Friis's transmission formula can be derived as

$$P_r = P_t G_t(\theta, \psi) G_r(\theta, \psi) \left(\frac{\lambda}{4\pi d} \right)^2,$$

where P_t is transmitted power, P_r is received power, $G_t(\theta, \psi)$ is the function of the gain of the transmitting antenna with θ and ψ representing an elevation and azimuth angle, in the direction of the receiving antenna, $G_r(\theta, \psi)$ is the function of the gain of the receiving antenna with θ and ψ , an elevation and azimuth, in the direction of the transmitting antenna, λ is a wavelength, d is a distance between the transmitter and the receiver antenna.

It seems that the shorter wavelength causes a higher loss in mmWave than in sub-6 GHz. However, this is not the case if we consider the effective area of the receiver antenna. The effective area of the antenna is

$$A = \frac{\lambda^2}{4\pi}.$$

Then Friis's formula can be rewritten as

$$P_r = P_t G_t(\theta, \psi) G_r(\theta, \psi) \left(\frac{A}{4\pi d^2} \right),$$

where there is no λ , carrier frequency, in the equation. This means that there is no difference in loss in different frequencies if the effective area of the antenna is fixed.

In the test setup, the UE is located at a certain distance with a very small variation in distance, d . The effective area of the receiver antenna is also fixed. The angle of the transmitting and receiving antennas θ and ψ vary depending on the position of the gimbal. This will be considered as part of the features of the model.

5.3 Different Methods in UE Power Modeling

The purpose of UE power modeling is to estimate the UE power consumption in different scenarios of radio parameters and physical positions, that is, orientation. There are three test schemes: uplink and downlink power sweep, and horizontal orientation. The above cases are performed on different connection schemes and different MCS. The UE power is a target variable, also called a dependent variable, while the rest of the parameters are features, also called independent variables, as shown in Figure 5.4. The description of each measured parameter is described in Table 5.1.

In this thesis, three different methods of UE power modeling are studied, namely: polynomial regression, decision tree regression, and neural network.

Table 5.1: Target and features and description

Variables	Short description
Target variable	
UE_PowerMeas	UE power in mW
Features	
H_degree	Orientation in degrees in the horizon
Lte_RSRP(dBm)	Reference signal received power in dBm in LTE
Lte_RSRQ(dB)	Reference signal received quality in dB in LTE
NR_RSRP(dBm)	Reference signal received power in dBm in NR
NR_RSRQ(dB)	Reference signal received quality in dB in NR
LTEULpwr (dBm)	UE (uplink) power in dBm in LTE
NRULpwr (dBm)	UE (uplink) power in dBm in NR
NRDLpwr (dBm)	UE (downlink) power in dBm in NR
DL_LteNack	% Negative acknowledge in DL in LTE
DL_LteDtx	% Discontinuous transmission in DL in LTE
DL_NrNack	% Negative acknowledge in DL in NR
DL_NrDtx	% Discontinuous transmission in DL in NR
UL_LteNack	% Negative acknowledge in UL in LTE
UL_LteDtx	% Discontinuous transmission in UL in LTE
UL_NrNack	% Negative acknowledge in UL in NR
UL_NrDtx	% Discontinuous transmission in UL in NR
UL_LteMCS	Modulation and coding scheme in UL in LTE
DL_LteMCS	Modulation and coding scheme in DL in LTE
UL_NrMCS	Modulation and coding scheme in UL in NR
DL_NrMCS	Modulation and coding scheme in DL in NR

Position	RF-modem	Independent variable (features)			Dependent variable (target variable)
		H-ARQ	MCS	UE power	
H_degree	UE received power	Uplink	Downlink	LTE	UE_PowerMeas (mW)
	Lte_RSRP(dBm)	DL_LteNack%	UL_LteNack%	UL_LteMCS	
	Lte_RSRQ(dBm)	DL_LteDtx%	UL_LteDtx%	DL_LteMCS	
	NR_RSRP(dBm)	DL_NrNack%	UL_NrNack%	NR	
	NR_RSRQ(dBm)	DL_NrDtx%	UL_NrDtx%	UL_NrMCS	
	NR_SINR(dBm)			DL_NrMCS	
	UE transmitted RF power	%BLER = (NACK+DTX)/(ACK+NACK+DTX)			
	LTEULpwr(dBm)				
	NRULpwr(dBm)				
	Base station transmitted RF power				
	NRDLpwr(dBm)				
	LTEDLpwr(dBm)				

Figure 5.4: Features and target variable.

5.4 Modeling in Idle Mode

In idle mode, UE consumes constant power over a long period of time. The measurement results are shown in the table in the previous chapter in the UE power measurement in idle mode. UE stays in idle mode until it responds to paging from the network or it initiates data request to the network. From there, UE switches to RRC_CONNECTED state and keeps the continuing schedule. Once there is no more data packet to schedule for a fixed period of time, it returns to idle mode. UE power in idle mode is denoted as P_{idle} .

5.5 Single Connectivity and Dual Connectivity Modeling in Connected Mode

Two connection types are considered in connected mode, namely: LTE-only as a single connectivity (only LTE is connected) and ENDC as a dual connectivity (both LTE and NR are connected).

5.5.1 Single and Multiple Features Polynomial Regression

Modeling of LTE-only Uplink Power Sweep

In this scheme, the UE is in a fixed position and only the LTE uplink power changes with a specific power range and interval. This scheme is done in three different positions: 0, 60 and 90 degrees in horizon. They can be modeled using a

single feature, LTE uplink power, and 6th order polynomial, as shown in Figures 5.5, 5.6 and 5.7.

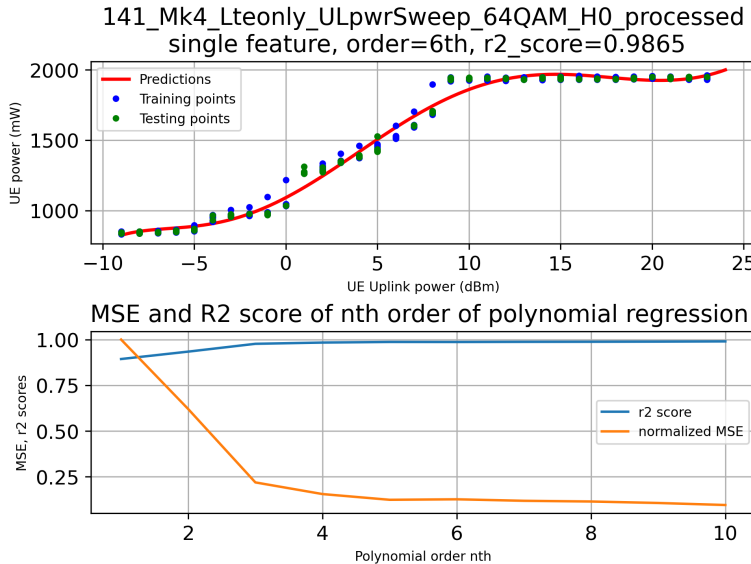


Figure 5.5: Single feature polynomial regression of LTE-only with UL power sweep with 64QAM at H = 0 degrees.

As in the results, the single feature fits well in this simple curve of power consumption with relatively good r2 score, hence multiple features regression is unnecessary in this scheme.

NR Uplink Power Sweep in ENDC

In this scheme, the UE is in a fixed position and only the NR uplink power changes with a specific power range and interval. This scheme is done in single position of 112 degrees in horizon. It can be modeled using a single feature, the NR uplink power, of 6th order polynomial regression, and the result is shown in Figure 5.8.

As in the result, the single feature fits well in this simple curve of power consumption with relatively good r2 score, hence multiple features regression is also unnecessary in this scheme.

NR Downlink Power Sweep in ENDC

In this scheme, the UE is in a fixed position and only the NR downlink power changes with a specific power range and interval. This scheme is done in single position of 112 degrees in horizon. It can be modeled using single feature, NR downlink power, of 6th order polynomial regression, and the result shows in Fig-

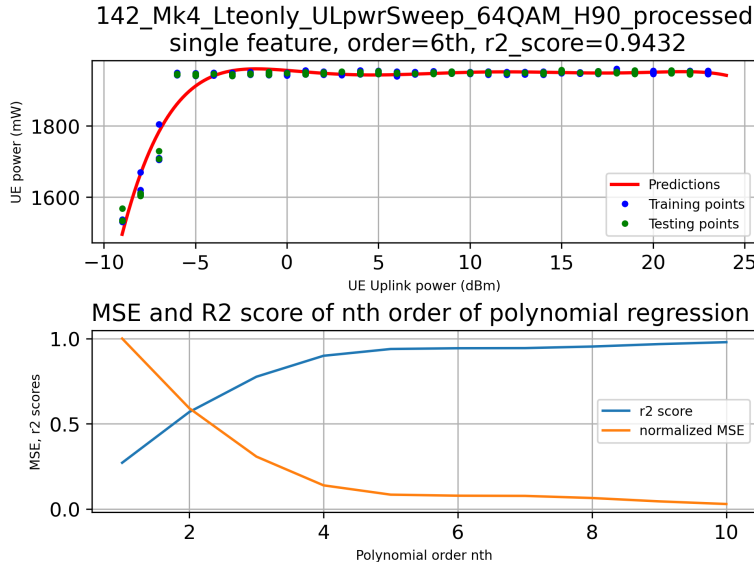


Figure 5.6: Single feature polynomial regression of LTE-only with UL power sweep with 64QAM at $H = 60$ degrees.

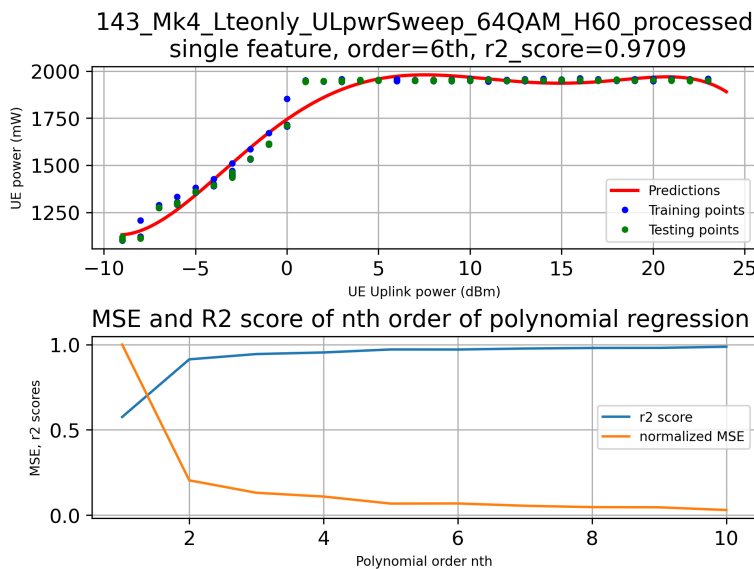


Figure 5.7: Single feature polynomial regression of LTE-only with UL power sweep with 64QAM at $H = 90$ degrees.

ure 5.9. However, the power curve is quite sharp and does not fit well in very low

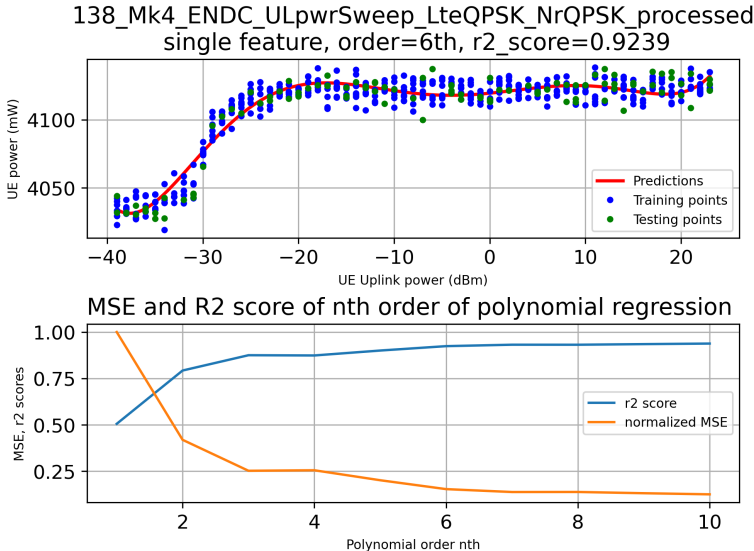


Figure 5.8: Single feature polynomial regression of ENDC with NR UL power sweep with NR-QPSK at $H = 112$ degrees.

power.

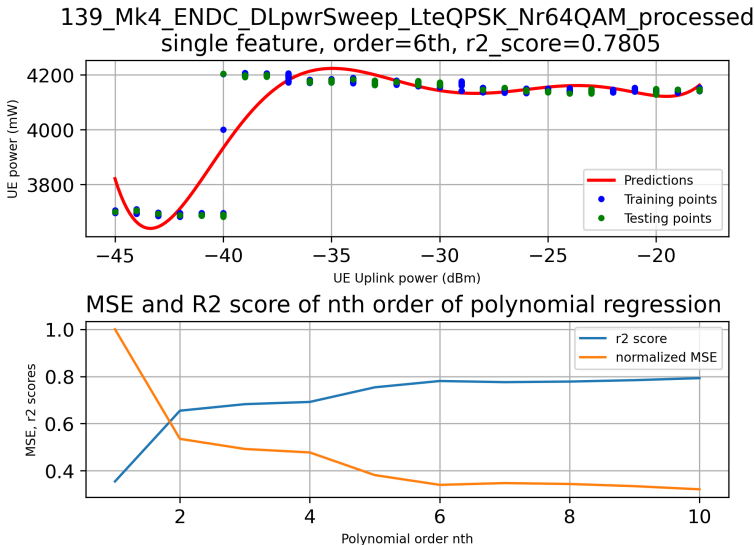


Figure 5.9: Single feature polynomial regression of ENDC with NR DL power sweep with NR-64QAM at $H = 112$ degrees.

In this case, multi-features polynomial regression is then used to improve the

prediction by adding high correlation coefficient features to the input X namely: NR_RSRQ (dBm), and NR_SINR (dBm). The result shows an improvement in prediction as in Figure 5.10.

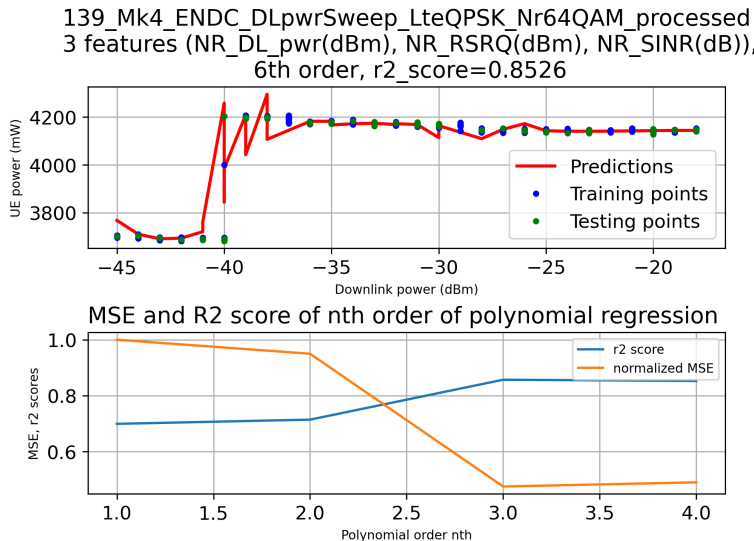


Figure 5.10: Multiple features polynomial regression of ENDC with NR UL power sweep with QPSK at $H = 112$ degrees.

5.5.2 Single and Multiple Features Using Decision Tree Regression

Figure 5.11 shows a single feature decision tree regression of the LTE-only uplink power sweep at $H = 0$ degrees.

A single feature decision tree regression of the NR uplink power sweep in ENDC at $H = 112$ is shown in Figure 5.12.

A single feature decision tree regression of NR downlink power sweep in ENDC at $H = 112$ degrees is shown in Figure 5.13.

A single feature decision tree regression of the horizontal sweep in LTE-only between $H = -180$ and 180 degrees with QPSK is shown in Figure 5.14.

A single feature decision tree regression of horizontal sweep in LTE-only between $H = -180$ and 180 degrees with 64QAM is shown in Figure 5.15.

A single feature decision tree regression of horizontal sweep in ENDC between $H = 0$ and 180 degrees with LTE-64QAM and NR-QPSK is shown in Figure 5.16.

A single feature decision tree regression of the horizontal sweep in ENDC between $H = 0$ and 180 degrees with LTE-64QAM and NR-64QAM is shown in Figure 5.17.

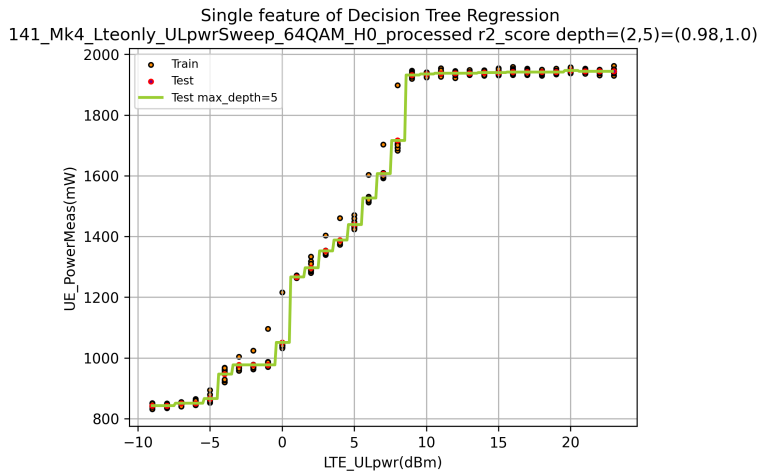


Figure 5.11: A single feature decision tree regression of LTE-only uplink power sweep at $H = 0$ degrees.

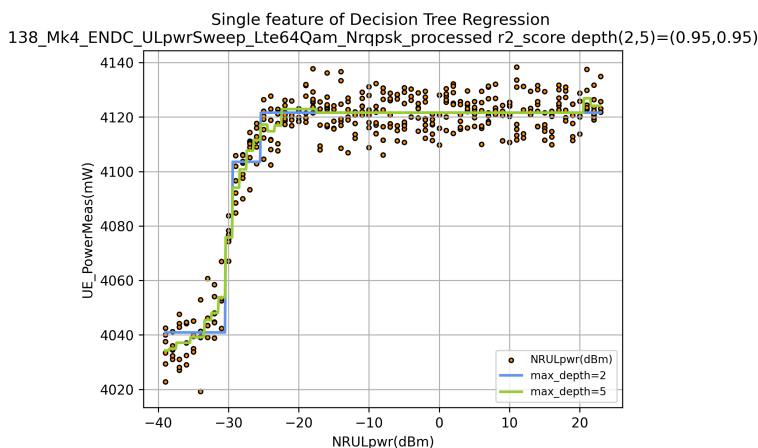


Figure 5.12: A single feature decision tree regression of LTE-only uplink power sweep at $H = 112$ degrees.

Decision tree regression gives quite good performance in the results given only with a single feature and depths of 5 and 7. However, it can be insufficient when there are multiple high correlation coefficients in the dataset. The Multiple features decision tree regression is then used and is shown in the following figures.

Multiple features, three features, decision tree regression of horizontal sweep in LTE-only between $H = -180$ and 180 degrees with QPSK is shown in Figure 5.18.

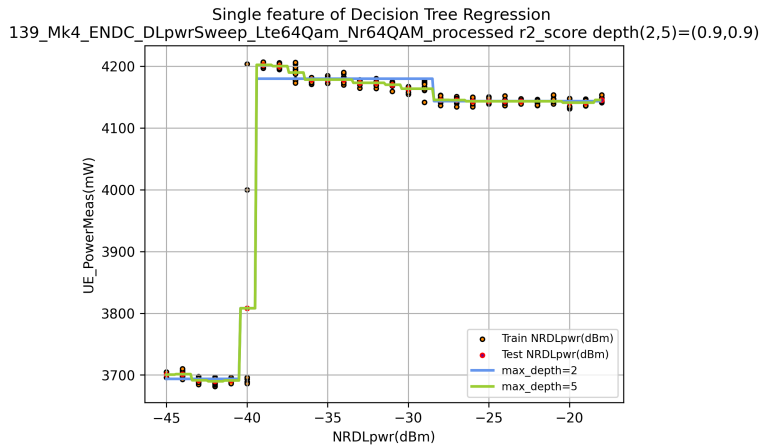


Figure 5.13: A single feature decision tree regression of LTE-only uplink power sweep at $H = 112$ degrees.

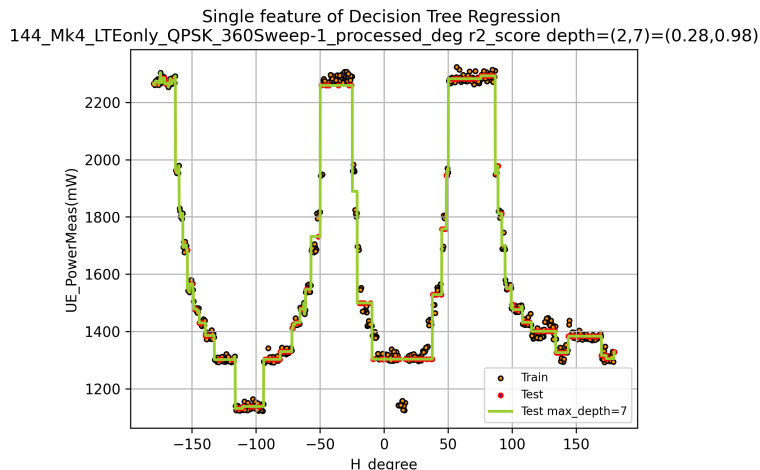


Figure 5.14: A single feature decision tree regression of horizontal sweep in LTE-only between -180 and 180 degrees in horizon with QPSK.

Multiple features, three features, decision tree regression of horizontal sweep in ENDC between $H = 0$ and 180 degrees with LTE-64QAM and NR-QPSK is shown in Figure 5.19.

The performance improvement with multiple features in decision tree regression is relatively small, hence seem non-necessary for multiple features. In general, decision tree regression gives quite good estimation and is versatile for different kinds of graph pattern.

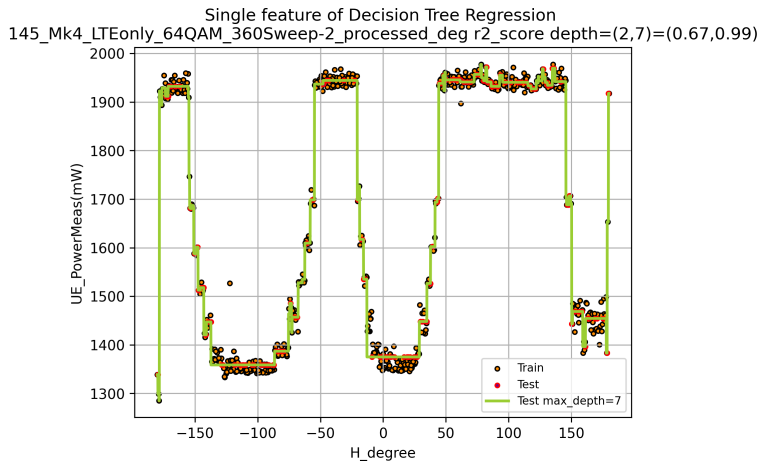


Figure 5.15: A single feature decision tree regression of horizontal sweep in LTE-only between -180 and 180 degrees in horizon with 64QAM.

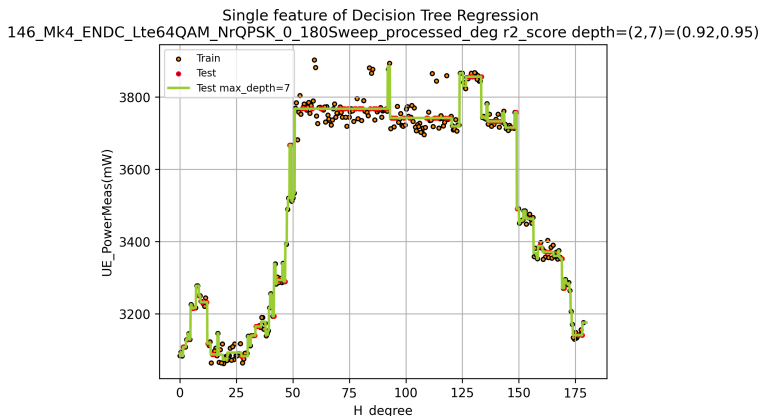


Figure 5.16: A single feature decision tree regression of horizontal sweep in ENDC between 0 and 180 degrees in horizon with LTE-64QAM and NR-QPSK.

5.5.3 Multiple Features Using Neural Network

The results using the deep neural network will be listed by cases below.

Multiple features, three features, the neural network of the LTE uplink power sweep with LTE-only at $H = 0$ degrees with LTE-64QAM is shown in Figure 5.20. The loss function for the same case is shown in 5.21.

Multiple features, three features, the neural network of the NR uplink power sweep with ENDC at $H = 112$ degrees with LTE-QPSK and NR-QPSK is shown in

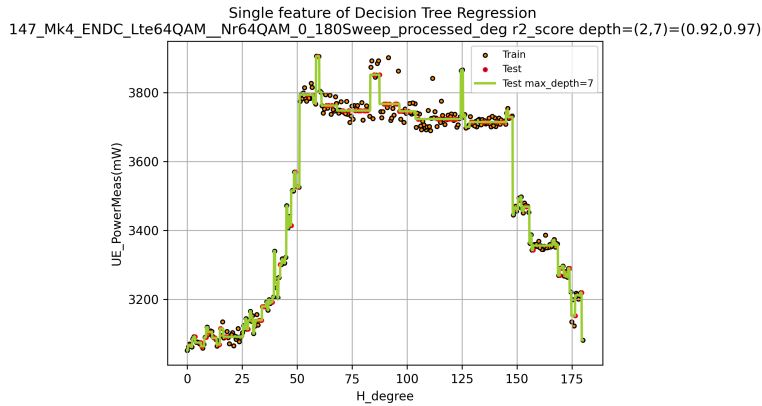


Figure 5.17: A single feature decision tree regression of horizontal sweep in ENDC between 0 and 180 degrees in horizon with LTE-64QAM and NR-64QAM.

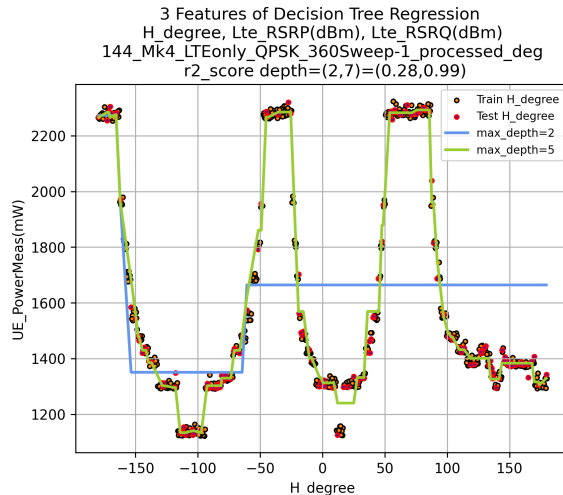


Figure 5.18: A multiple features decision tree regression of horizontal sweep in LTE-only between -180 and 180 degrees in horizon with QPSK.

Figure 5.22. The loss function for the same case is shown in 5.23.

Multiple features, four features, the neural network of NR downlink power sweep with ENDC at $H = 112$ degrees with LTE-QPSK and NR-64QAM is shown in Figure 5.24. The loss function for the same case is shown in 5.25.

Multiple features, four features, the neural network of horizontal sweep with LTE-only between $H = -180$ to 180 degrees with QPSK is shown in Figure 5.24. The loss function for the same case is shown in 5.25.

Multiple features, four features, the neural network of horizontal sweep with

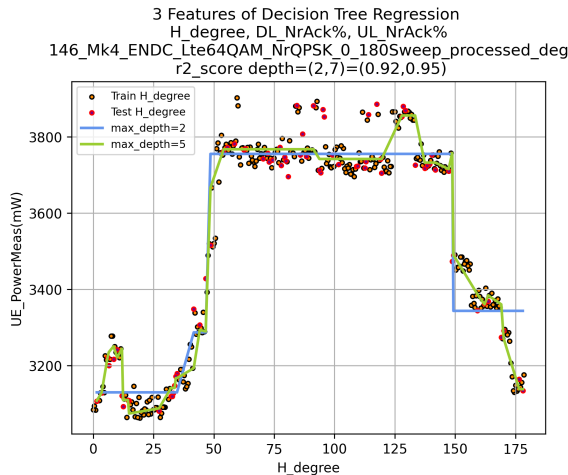


Figure 5.19: A multiple features decision tree regression of horizontal sweep in ENDC between 0 and 180 degrees in horizon with LTE-64QAM and NR-QPSK.

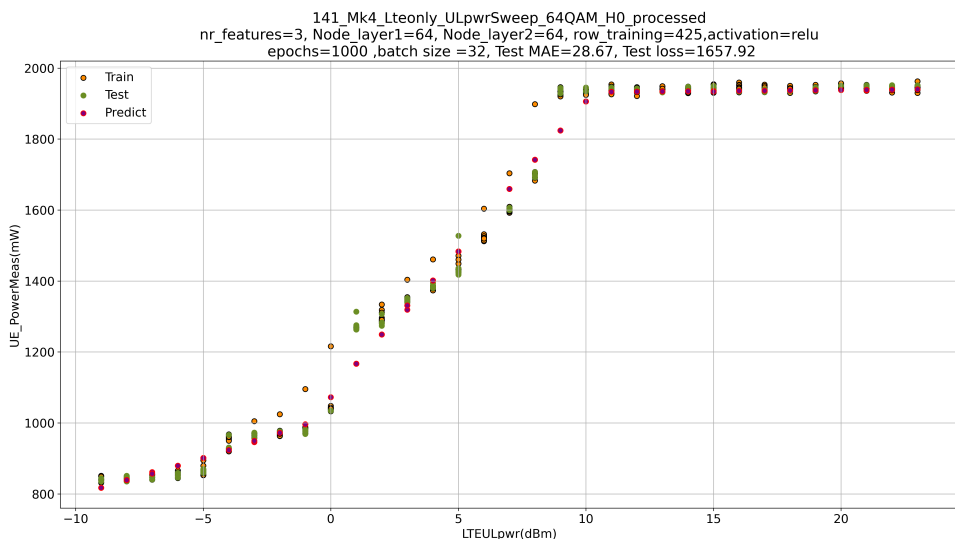


Figure 5.20: A multiple features neural network of LTE uplink power sweep in LTE-only between 0 and 180 degrees in horizon with LTE-64QAM.

LTE-only between $H = -180$ to 180 degrees with 64QAM is shown in Figure 5.28. The loss function for the same case is shown in 5.29.

Multiple features, four features, the neural network of horizontal sweep with ENDC between $H = 0$ and 180 degrees with LTE-64QAM and NR-QPSK is shown

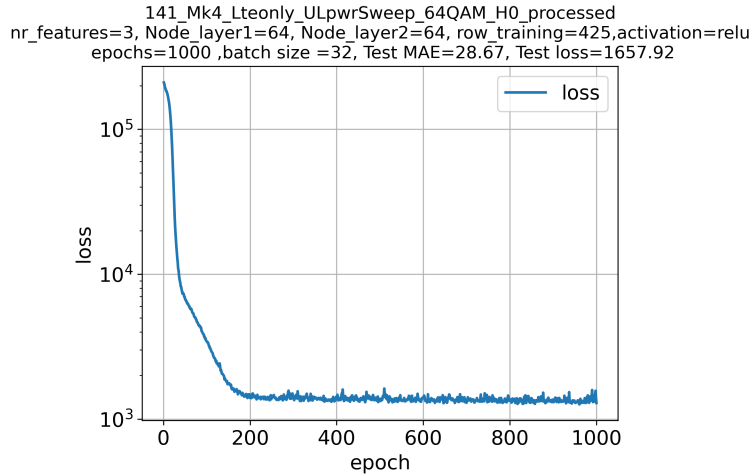


Figure 5.21: A loss of a multiple features neural network of LTE uplink power sweep in LTE-only between 0 and 180 degrees in horizon with LTE-64QAM.

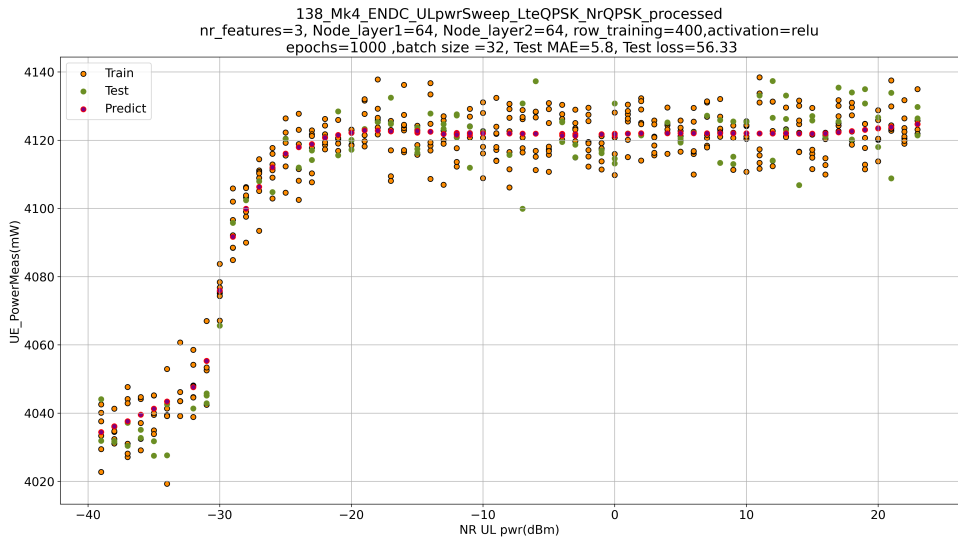


Figure 5.22: A multiple features neural network of NR uplink power sweep in LTE-only between 112 and 180 degrees in horizon with LTE-QPSK and NR-QPSK.

in Figure 5.30. The loss function for the same case is shown in 5.31.

Multiple features, four features, the neural network of the horizontal sweep of UE with ENDC between H = 0 and 180 degrees with LTE-64QAM and NR-

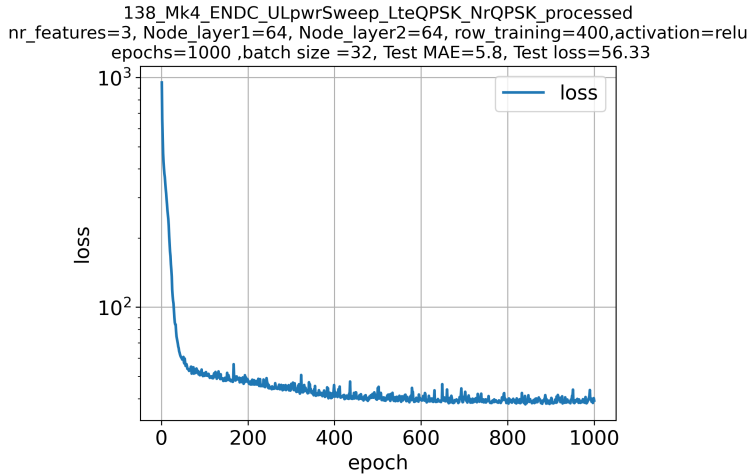


Figure 5.23: A multiple features neural network of NR uplink power sweep in LTE-only between 112 and 180 degrees in horizon with LTE-QPSK and NR-QPSK.

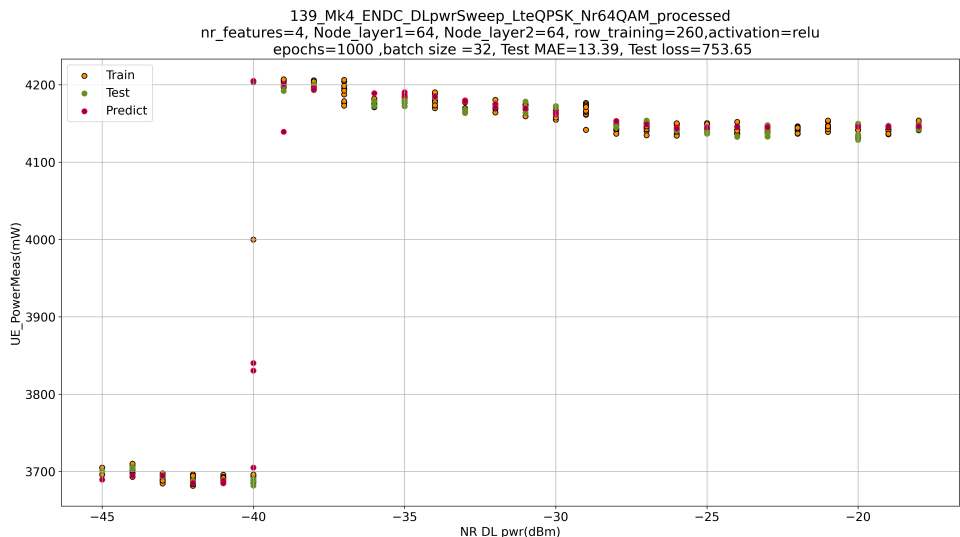


Figure 5.24: A multiple features neural network of NR downlink power sweep in LTE-only between 112 and 180 degrees in horizon with LTE-QPSK and NR-64QAM.

64QAM is shown in Figure 5.32. The loss function for the same case is shown in 5.33.

The deep neural network, in general, gives quite reasonably good results in

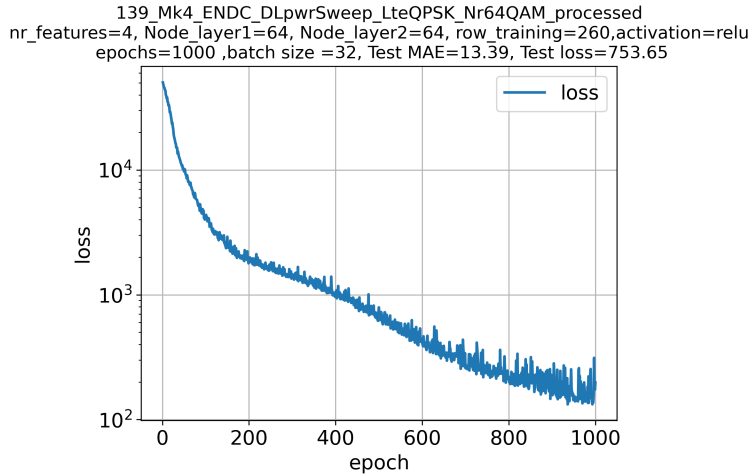


Figure 5.25: A multiple features neural network of NR downlink power sweep in LTE-only between 112 and 180 degrees in horizon with LTE-QPSK and NR-64QAM.

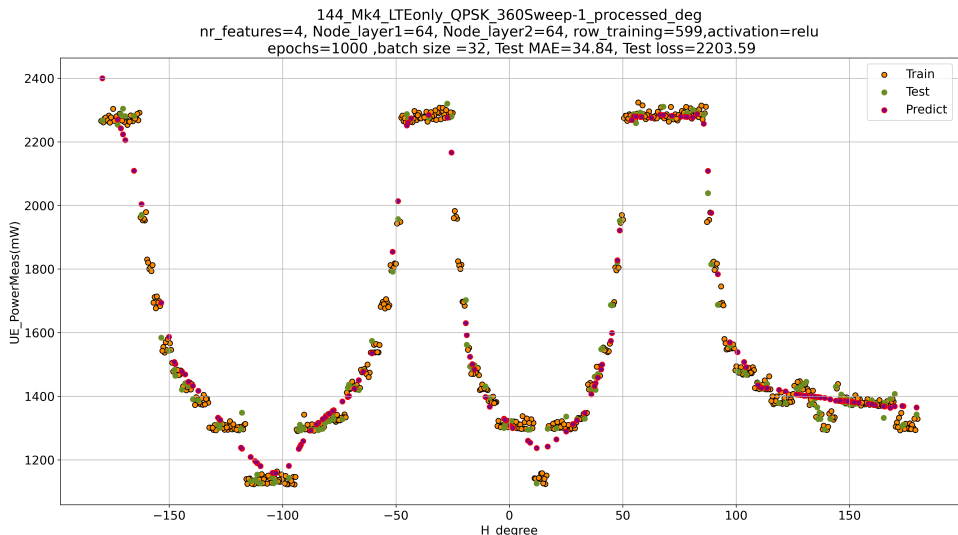


Figure 5.26: A multiple features neural network of UE horizontal sweep in LTE-only between -180 and 180 degrees in horizon with LTE-QPSK.

terms of MAE. However, this mainly depends on the number of iterations in the training and the amount of training data. More training iterations usually lead to lower loss, but it could also lead to the point that it is over-fitted.

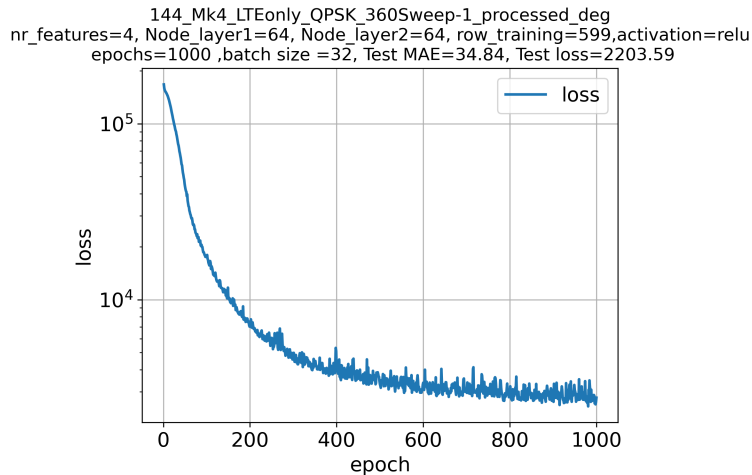


Figure 5.27: A loss function of a multiple features neural network of NR downlink power sweep in LTE-only between -180 and 180 degrees in horizon with LTE-QPSK.

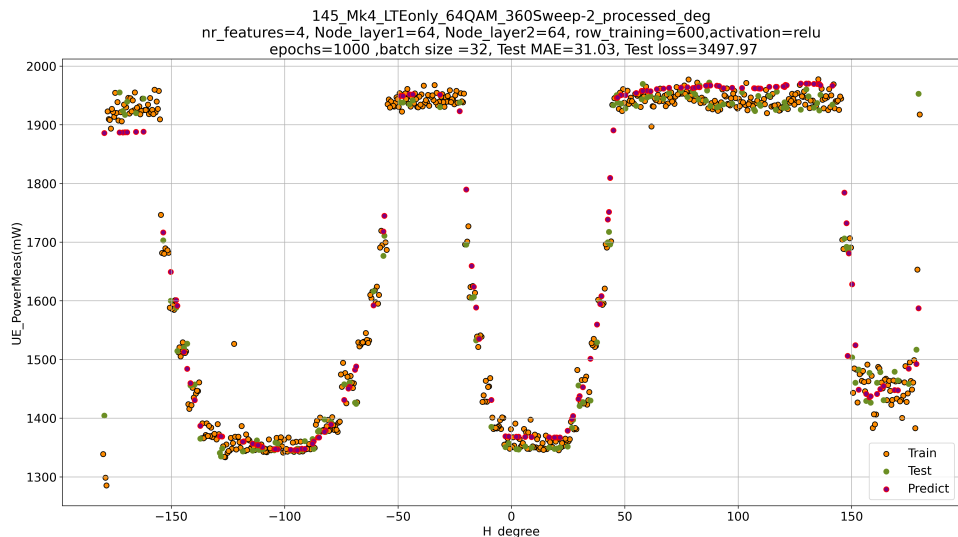


Figure 5.28: A multiple features neural network of UE horizontal sweep in LTE-only between -180 and 180 degrees in horizon with 64QAM.

5.6 Prediction System

The prediction system can be built by combining pre-trained models. By conditioning the connection mode, the model can be properly selected for the prediction of UE power. The prediction system can then be created as shown in Figure

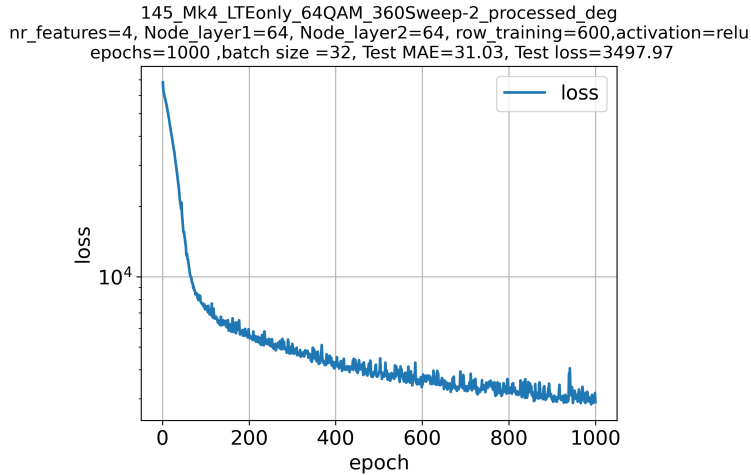


Figure 5.29: A loss function of a multiple features neural network of NR downlink power sweep in LTE-only between -180 and 180 degrees in horizon with 64QAM.

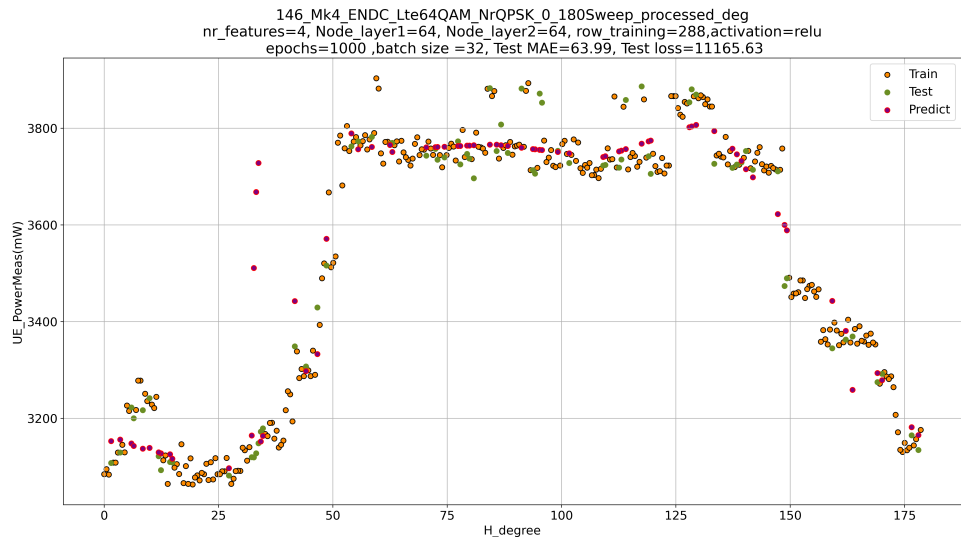


Figure 5.30: A multiple features neural network of UE horizontal sweep in ENDC between 0 and 180 degrees in horizon with LTE-64QAM and NR-QPSK.

5.34, where X is an input vector that contains features, P_{idle} is the function of the idle mode power with the paging cycle as input, P_{CON_LTE} is the function of connected mode (LTE-only) power with distance (d), MCS and ψ_h as input and

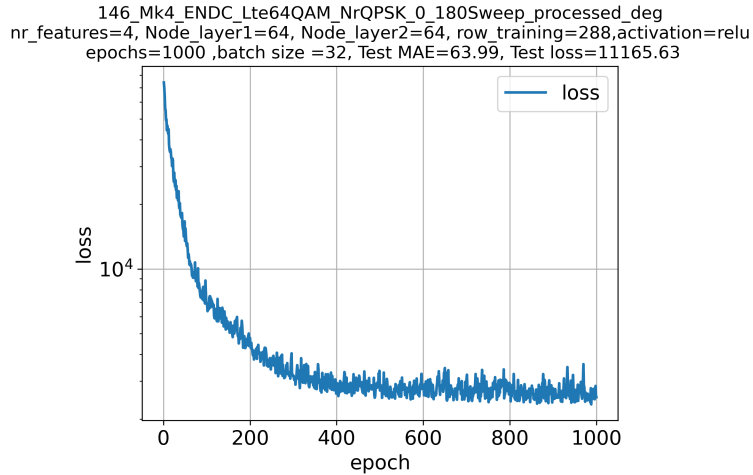


Figure 5.31: A loss function of a multiple features neural network of NR downlink power sweep in ENDC between 0 and 180 degrees in horizon with LTE-64QAM and NR-QPSK.

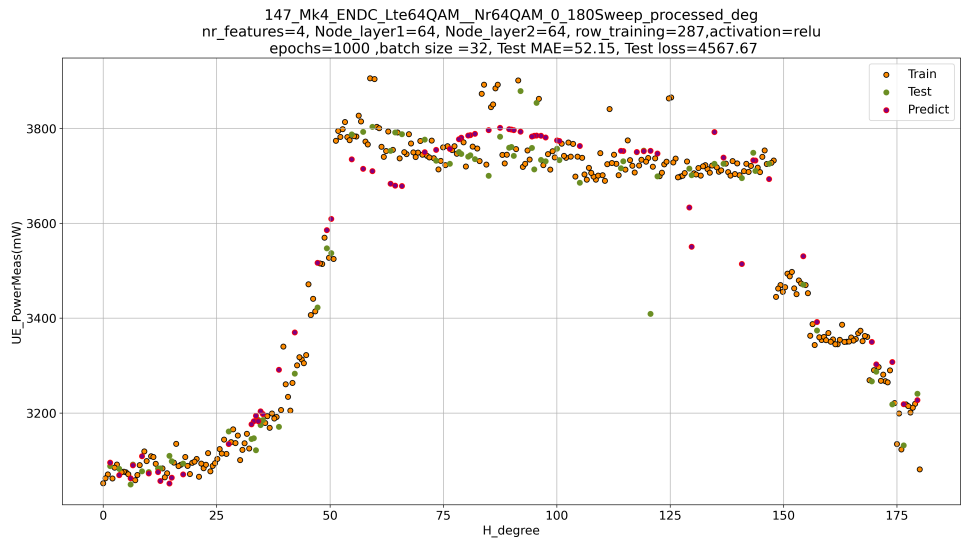


Figure 5.32: A multiple features neural network of UE horizontal sweep in ENDC between 0 and 180 degrees in horizon with LTE-64QAM and NR-64QAM.

P_{CON_ENDC} is the function of connected mode (ENDC) power with distance (d), MCS of LTE and NR and ψ_h as input. Decision tree regression or neural networks can be used as a model in the prediction system mainly because the pre-trained

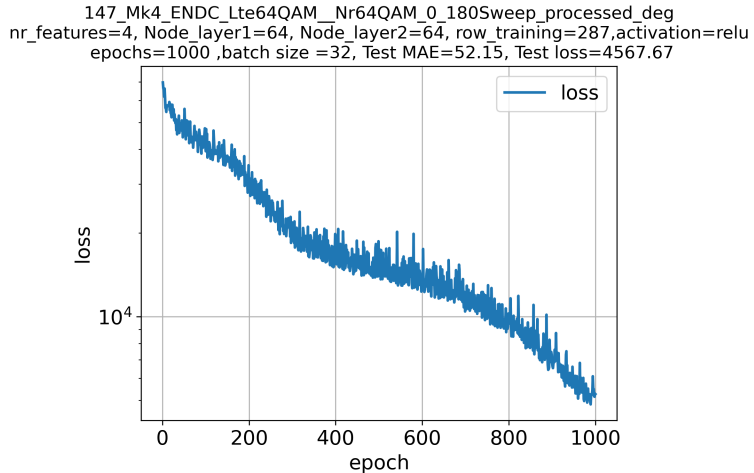


Figure 5.33: A loss function of a multiple features neural network of NR downlink power sweep in ENDC between 0 and 180 degrees in horizon with LTE-64QAM and NR-64QAM.

models are available in most cases of connection mode and MCS.

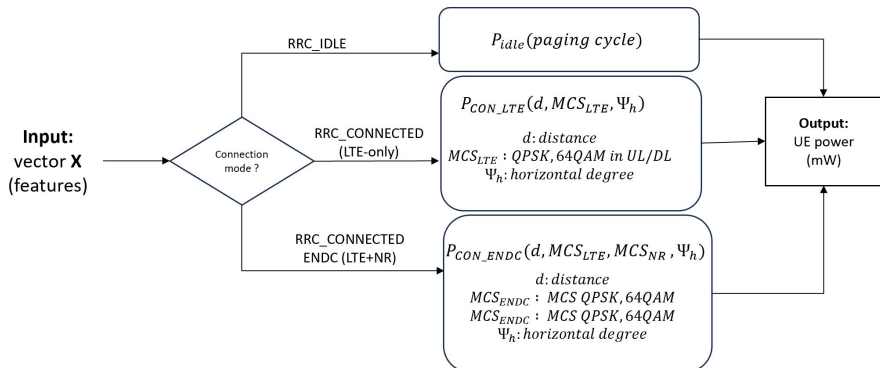


Figure 5.34: A prediction system.

6

Results

Some observations were found in the measured data. In LTE-only, QPSK consumes substantially more power than 64QAM, while in NR, UE consumes a similar amount of power across different MCSs in NR. In addition, in ENDC, UE has a relatively small variation in power for a specific MCS when it successfully transmitted packets without, or small, BLER. There are unique patterns of UE power in the orientation sweep in LTE. It is influenced by factors such as antenna gain, selection and combining within each scheme (a certain MCS, connection mode, and distance from the base station). UE consumes more power when there is a high percentage of NACK but relatively low when there is a high percentage of DTX in the downlink, this could be the reason that DTX does not require processing for decoding while UE need to first decode the packet and realized that it is wrongly decoded as NACK. There is fixed ceiling power in the UE (power budget) for a certain MCS and connection mode. The power budget, the ceiling power can be shown in Table 6.2.

Three modeling methods were investigated and tested. The performance of all models in each scheme can be seen in Table 6.1. The blank cells are those cases that are not feasible or not necessary.

Table 6.1: A table comparing the performance of different modeling methods in different schemes.

Performance	Polynomial regression 1-feature	Polynomial regression multi-features	Decision tree regression 1-feature	Decision tree regression multi-features	Neural network multi-feature
LTE-only: LTE UL power sweeping	Order = 6, r2_score = 0.98	-	Depth = 5, r2_score ~= 1	-	MAE (Mean absolute error) = 27
LTE-only: orientation sweeping	-	-	Depth = 7, r2_score = 0.98	Depth = 7, r2_score = 0.99	MAE = 35
ENDC: NR UL power sweeping	Order = 6, r2_score = 0.92	-	Depth = 5, r2_score = 0.95	-	MAE = 6
ENDC: NR DL power sweeping	Order = 6, r2_score = 0.78	Order = 6, r2_score = 0.85	Depth = 5, r2_score = 0.9	-	MAE = 13
ENDC: orientation sweeping	-	-	Depth = 7, r2_score = 0.95	Depth = 7, r2_score = 0.95	MAE = 64

Table 6.2: A table shows power budget for each connection mode and MCS.

Schemes	Ceiling power (mW)
LTE-only QPSK	2285
LTE-only 64QAM	1950
ENDC: LTE-QPSK, NR-QPSK or NR-64QAM	4200
ENDC: LTE-64QAM, NR-QPSK or NR-64QAM	3750

7

Conclusion

7.1 Findings in Modeling

These are findings for the three modeling methods.

Firstly, the polynomial regression is studied with UE UL Tx power sweep cases. This is because polynomial regression works well with a simple curve. The estimation parameters can be stored in the form of a bias vector, β , and can be exploited by simply plugging in all the input variables in all the combinatorial terms depending on how many features and in what order. In the case of multiple features, more than one highly correlated feature, the performance is then boosted, i.e., DL Tx power sweeping in NR. Polynomial regression can be beneficial for the learning characteristic of the PA in the UE.

Secondly, the decision tree regression performs quite well in all schemes with a single feature. However, having multiple features in the decision tree regression could improve prediction in terms of robustness. The additional features need to be carefully selected based on the statistical data. The decision tree model can be stored and loaded again in the prediction system.

Thirdly, the deep neural network also performs well in all test schemes using multiple features. This method is also quite versatile. However, to achieve robustness and low loss, more training data is required.

Finally, the prediction system can be built by combining all test schemes in which the input is a vector of features. The submodel is chosen on the basis of the UE connection mode, MCS, and orientation. Decision tree regression or neural networks can be used as submodels in the prediction system mainly because the pre-trained submodels are available in most cases of connection mode and MCS.

However, the prediction system heavily relies on the pre-trained models as input. This requires a lot of training data and a complete matrix of all possible

cases, i.e., the full range of all possible combinations of variable values. Moreover, the models are dependent on a specific UE, namely the Sony Xperia Mark 4. In this thesis, the insights from each parameter are investigated, and they are more or less independent of the UE model.

7.2 Discussion

This section will discuss the research questions and further research.

7.2.1 Research Questions

How can features be selected for each test scheme, and will that improve the models with more features?

A primary feature can be selected based on the varying parameter in each test scheme. For example, in the UL RF power sweep, the UL RF power is the varying parameter. Therefore, the UL RF power is the main parameter and if there are few parameters that have Pearson correlation coefficient greater than around 0.4 in the whole data series, including a few features improves performance.

What is the performance of each modeling method in each test scheme?

The performance for each modeling method according to each test scheme can be found in the section 7.1.

How can one build a potential prediction system for 5G UE power consumption?

The prediction system is suggested in section 5.6.

7.2.2 Further Research

This section discusses further research that could be investigated beyond the scope of this thesis.

Energy Efficiency in Separate UL and DL Direction

The Energy Efficiency (EE), which is the amount of energy required to transmit or receive a byte of data (Joule/byte), can be investigated in each transmission direction: UL and DL. In this thesis, both UL and DL are active in all test cases in connected mode, which makes EE not very useful due to the mixture of UL and DL throughput. The distribution of UL and DL throughput is based on the MCS index and radio frame configuration, i.e., the ratio between UL and DL symbols in the radio frame. Therefore, further research focusing on the EE of separated

UL or DL is beneficial for understanding the EE in each direction and will provide insights into the power consumption of the UL and DL RF chains.

Using Random Forest to Enhance Decision Tree Regression

A random forest can be explored to model UE power consumption. The random forest is a modeling method for solving regression tasks that is built by assembling multiple decision trees from random data subsets. The final prediction is determined by averaging all the tree predictions. This method could reduce overfitting and improve robustness and accuracy because the dataset sometimes exhibits various behaviors, such as high block error rate (BLER) from NACK or high BLER from DTX.

Bibliography

- [1] Rodrigo D. Alfaia, Bruno S. Da Silva, Anderson F. Souto, and Ana M. Schramm. User equipment power consumption analysis for configurable bandwidth part (bwp) in a 5g network. In *2023 IEEE Colombian Caribbean Conference (C3)*, pages 1–5, 2023. doi: 10.1109/C358072.2023.10436302.
- [2] Robert Falkenberg, Benjamin Sliwa, and Christian Wietfeld. Rushing full speed with lte-advanced is economical - a power consumption analysis. In *2017 IEEE 85th Vehicular Technology Conference (VTC Spring)*, pages 1–7, 2017. doi: 10.1109/VTCSpring.2017.8108515.
- [3] Pål Frenger, Peter Moberg, Jens Malmomin, Ylva Jading, and Istvan Godor. Reducing energy consumption in lte with cell dtx. In *2011 IEEE 73rd Vehicular Technology Conference (VTC Spring)*, pages 1–5, 2011. doi: 10.1109/VETECS.2011.5956235.
- [4] Anders R. Jensen, Mads Lauridsen, Preben Mogensen, Troels B. Sørensen, and Per Jensen. Lte ue power consumption model: For system level energy and performance optimization. In *2012 IEEE Vehicular Technology Conference (VTC Fall)*, pages 1–5, 2012. doi: 10.1109/VTCFall.2012.6399281.
- [5] Mads Lauridsen, Gilberto Berardinelli, Troels B. Sorensen, and Preben Mogensen. Ensuring energy efficient 5g user equipment by technology evolution and reuse. In *2014 IEEE 79th Vehicular Technology Conference (VTC Spring)*, pages 1–6, 2014. doi: 10.1109/VTCSpring.2014.7022914.
- [6] Yu-Ngok Ruyue Li, Mengzhu Chen, Jun Xu, Li Tian, and Kaibin Huang. Power saving techniques for 5g and beyond. *IEEE Access*, 8:108675–108690, 2020. doi: 10.1109/ACCESS.2020.3001180.

Index

CA	PA
abbreviation, ix	abbreviation, ix
CRS	RF
abbreviation, ix	abbreviation, ix
DL	RRC
abbreviation, ix	abbreviation, ix
DRX	3GPP
abbreviation, ix	abbreviation, ix
DUT	UE
abbreviation, ix	abbreviation, ix
ENDC	UL
abbreviation, ix	abbreviation, ix
5G	
abbreviation, ix	
5GCN	
abbreviation, ix	
FR2	
abbreviation, ix	
LNA	
abbreviation, ix	
LTE	
abbreviation, ix	
MCS	
abbreviation, ix	
MMWAVE	
abbreviation, ix	
NR	
abbreviation, ix	